The Nucleus Reuniens Drives Hippocampal Goal-directed Trajectory Sequences for Route Planning

Dissertation
zur Erlangung des Doktorgrades
der Naturwissenschaften

vorgelegt beim Fachbereich Biowissenschaften
der Johann Wolfgang Goethe-Universität
in Frankfurt am Main

von
Hye-A Kim
aus Seoul, Südkorea

Frankfurt am Main 2023
(D 30)

vom Fachbereich Biowissenschaften der

Johann Wolfgang Goethe - Universität als Dissertation angenommen.

Dekan:	Prof. Dr. Sven Klimpel
Gutachter:	Prof. Dr. Manfred Kössl
	Dr. Hiroshi Ito
Datum der Disputation:	March 11, 2024

Acknowledgments

First and foremost, I would like to express my sincere appreciation to my direct supervisor Dr. Hiroshi Ito for all the support. It has been a great pleasure for me to carry out this challenging but very exciting project within the new starting group, under the guidance of a supportive, passionate, and brilliant supervisor. Whenever I had a concern about something, a meeting with Hiroshi just cleared up all the issues and gave me the direction to pursue. Not only as a supervisor, I respect Hiroshi as a person and a neuroscientist, and I am grateful to have learned a lot from him over the years.

I appreciate Prof. Dr. Manfred Kössl for being my supervisor and for giving me valuable advice whenever I meet him. The letter of recommendation I've received and the references for writing the thesis mean a lot to me. I would also like to thank Prof. Dr. Pascal Fries for being my thesis advisor and always helping me with my project and my future career.

I would like to thank all the current and former members of the Ito lab for their support. Especially to Raunak, Joeri, and Norihiro for giving me lots of advice and help whenever I needed it and for inspiring me in neuroscience. Sincere thanks to Shao-Fang and Robert for helping me with the experiment. Thanks to Zahra and Alessa for being a good friend and not just a colleague.

Many thanks to the current and former graduate program coordinators, Arjan, Irina, and Silke. Their support of the students in various aspects, including hosting TAC meetings and providing information from registration

to university to graduation, is a very valuable help. I would also like to thank the imaging facility team, Florian, Stephan, and Christine, for their continuous efforts in supporting us to have a good image more easily. Without the help of the animal facility team, it would be very difficult to do the animal experiment. Thanks to Emily, Nina, Silke, and other animal caretakers for their great support in maintaining good living conditions for the rats and animal welfare.

Thanks to all the animals I experimented with or contributed to the project and were sacrificed. I deeply regret any pain I may have caused you, and please know that it was never intentional. I hope you enjoyed your time with me and wish you a peaceful afterlife beyond the laboratory.

Finally, I would like to thank my entire family, including Gyubin, Sua, my mother Youngsuk, my father Seongsik, Juhan, and my grandmothers who passed away while I was in Germany. I could not even start my adventure without your belief and support, and it was the engine for me all the time. Especially to my partner Juhan, who always encouraged and motivated me with his love to get up and run again. My little dog Pearl, it has been a very hard time since you left. Walking with you and your smile has been the number one cure for me whenever I felt down or depressed. Thank you for everything you have given me and I love you forever and ever.

Table of Contents

List of Figures

Chapter 3.

Chapter 4.

Chapter 5.

Abstract

Goal-directed spatial navigation requires accurate estimates of one's position and destination, as well as careful planning of a route between them to avoid known obstacles in the environment. Despite its general importance across species, the neural circuitry supporting the ability for route planning remains largely unclear. Previous studies described that place cells in the hippocampal CA1 encode the animal's next movement direction (Wood et al., 2000; Ito et al., 2015) and upcoming navigational routes (Pfeiffer & Foster, 2013). However, it has been shown that part of the CA1 activity representing the animal's future behaviors is not necessarily generated in the hippocampus, but is derived from the medial prefrontal cortex (PFC) via the nucleus reuniens of the thalamus (RE) (Ito et al., 2015). Notably, the importance of the PFC in navigation has been demonstrated in several studies, including the recent finding of a goal map in the orbitofrontal cortex (Basu et al., 2021). Therefore, I hypothesized that information flow from the PFC to CA1 via the RE plays a key role in route planning.

To assess the animals' route planning ability, I designed a new navigation task in which a rat has to navigate to a fixed target location from various starting positions in an arena. Furthermore, by adding an L-shaped wall in the maze and removing all light sources in the experimental room, this task forced the animals to plan a wall-avoiding route without relying on direct sensory perceptions. I confirmed that rats could learn this task successfully, memorizing the wall location and taking a smooth wall-avoidance route. To test the role of the RE, I inactivated RE neurons by expressing the inhibitory opsin SwiChR++, which resulted in a significant deficit in the animal's route planning ability, taking a longer non-smooth path to the destination. By contrast, this manipulation did not affect navigation performance when a straight goal-directed route was available, suggesting a specific role of the RE in route planning. I further found that DREADDs-mediated inactivation of neurons in the bilateral hippocampi resulted in a similar deficit in route planning ability, implying cooperation between the RE and the hippocampus. I finally examined the activity of hippocampal CA1 neurons with and without RE inactivation. While neurons in the hippocampus exhibited brief trajectory sequences corresponding to the animal's subsequent goal-directed journey, I found that this goal-directed bias of trajectory events was significantly reduced by RE inactivation, likely associated with route-planning deficits in these animals.

Altogether, this dissertation demonstrates the role of the RE from both behavioral and neural coding perspectives, identifying a pivotal circuit element supporting the animal's route-planning ability.

Zusammenfassung

Die zielgerichtete räumliche Navigation erfordert genaue Schätzungen der eigenen Position und des Ziels sowie eine sorgfältige Planung der Route zwischen diesen beiden Punkten, um bekannten Hindernissen in der Umgebung auszuweichen. Trotz ihrer allgemeinen Bedeutung bei allen Tierarten sind die neuronalen Schaltkreise, die die Fähigkeit zur Routenplanung unterstützen, noch weitgehend unklar. Frühere Studien haben gezeigt, dass Ortszellen im CA1 des Hippocampus die nächste Bewegungsrichtung des Tieres und bevorstehende Navigationsrouten kodieren. Es konnte jedoch gezeigt werden, dass ein Teil der CA1-Aktivität, die das zukünftige Verhalten des Tieres repräsentiert, nicht notwendigerweise im Hippocampus entsteht, sondern vom medialen präfrontalen Kortex (PFC) über den Nucleus reuniens des Thalamus (RE) abgeleitet wird. Die Bedeutung des PFC für die Navigation wurde in mehreren Studien nachgewiesen, unter anderem durch die kürzliche Entdeckung einer Zielkarte im orbitofrontalen Kortex. Daher habe ich die

Hypothese aufgestellt, dass der Informationsfluss vom PFC über den RE zum CA1 eine Schlüsselrolle bei der Routenplanung spielt.

Die Rolle des Nucleus Reuniens bei der Planung einer Hindernis-vermeidenden Route zu einem erinnerten Ziel

Um die kausale Rolle des RE zu testen, habe ich eine optogenetische Methode angewandt, indem ich das inhibitorische Opsin SwiChR++ exprimiert habe, um die Aktivität der RE-Neuronen während der Reise zum Ziel zu unterdrücken. Um die Fähigkeit der Tiere zur Routenplanung zu testen, fügte ich dem Labyrinth eine L-förmige Wand hinzu und entfernte alle Lichtquellen aus dem Versuchsraum, um die Tiere zu zwingen, eine Route um die Wand herum zu planen, ohne sich auf direkte Sinneswahrnehmungen zu verlassen. Die Tiere wurden darauf trainiert, von verschiedenen Startpositionen zu einem festen Ziel zu navigieren, so dass wir die Fähigkeit der Tiere zur flexiblen Routenplanung testen konnten. Ich fand heraus, dass die Tiere mit abgeschaltetem RE häufig eine Route mit längerer Länge und Dauer wählten. Im Gegensatz dazu hatte diese Manipulation keinen Einfluss auf die Navigationsleistung, wenn eine geradlinige Route zur Verfügung stand, was auf eine spezifische Rolle des RE bei der Routenplanung hindeutet. Ich fand aber auch heraus, dass diese Tiere mit abgeschaltetem RE immer noch in der Lage waren, das richtige Ziel genau auszuwählen, was darauf hindeutet, dass die Beeinträchtigung nicht auf ein Defizit in der Zielerkennung zurückzuführen ist. Eine frühere Studie hat gezeigt, dass der RE eine Schlüsselstruktur ist, die Informationen über die zukünftige

Bewegungsrichtung des Tieres vom mPFC zum Hippocampus CA1 weiterleitet. Es ist daher möglich, dass Informationen über die Bewegungsrichtung im Hippocampus bei der Routenplanung in einem Labyrinth mit einem Hindernis hilfreich sein könnten. Um diese Idee weiter zu untersuchen, testete ich als Nächstes, wie sich die Inaktivierung von Neuronen im Hippocampus auf die Fähigkeit der Tiere zur Routenplanung auswirkt.

Die Deaktivierung der Neuronen im Hippocampus beeinträchtigt die Fähigkeit der Tiere, in einem vertrauten Labyrinth eine Route zu planen, aber nicht die Zielerkennung

Der Hippocampus wird als entscheidende Struktur für die räumliche Navigation angesehen, was jedoch nicht bedeutet, dass der Hippocampus für alle Aspekte des Navigationsverhaltens notwendig ist. Um die Rolle des Hippocampus bei der Navigation zu bestimmen, wählte ich einen chemogenetischen Ansatz, bei dem ich DREADDs verwendete, um die neuronale Aktivität im bilateralen Hippocampus zu hemmen. Zu meiner Überraschung war die Fähigkeit der Tiere, das richtige Ziel zu finden, auch nach der Inaktivierung der Neuronen im gesamten bilateralen Hippocampus nicht beeinträchtigt. Trotz der Tatsache, dass die Tiere in der Lage waren, das Ziel genau zu lokalisieren, führte die Inaktivierung des Hippocampus jedoch dazu, dass die Tiere einen längeren, verschlungenen Pfad einschlugen, was auf eine Beeinträchtigung der Fähigkeit zur Routenplanung hindeutet, wie sie bei Tieren mit RE-Inaktivierung beobachtet wurde. Im Gegensatz zu den

Fällen mit RE-Inaktivierung führte die Hippocampus-Inaktivierung jedoch nicht nur zu diesem Defizit, wenn die Wege von der geschlossenen Zone aus begannen, sondern auch, wenn sie von der offenen Zone aus begannen. Diese Beobachtung deutet darauf hin, dass das durch die Inaktivierung des Hippocampus hervorgerufene Verhaltensdefizit nicht auf die Planung des Weges zur Umgehung der Wand beschränkt ist. Zusammen mit früheren Studien über den menschlichen Hippocampus im Zusammenhang mit Orientierungspunkten deutet dieses Ergebnis darauf hin, dass der Hippocampus für die Erinnerung an Orientierungspunkte notwendig ist, was die Fähigkeit zur Routenplanung zur Vermeidung bekannter Hindernisse in der Umgebung unterstützen könnte. Meine nächste Frage betrifft die neuralen Mechanismen, mit denen der Hippocampus die Planung zukünftiger Navigationsrouten unterstützt. Um diese Frage zu beantworten, habe ich die Aktivität der Neuronen im Hippocampus aufgezeichnet, während das Tier die gleiche räumliche Navigationsaufgabe ausführte, und die Repräsentationen der Route im Hippocampus vor Beginn der Navigation analysiert.

Der Nucleus Reuniens steuert gezielte Ortszellaktivierungssequenzen im Hippocampus

Mehrere Studien haben gezeigt, dass die Ortszellen nicht nur die eigene Position des Tieres anzeigen, sondern manchmal auch den bevorstehenden Weg des Tieres zum nächsten Ziel darstellen, bevor es eine zielgerichtete Reise antritt. Da die Neuronen des RE in den Bereich CA1 des Hippocampus und in das Subiculum projizieren, vermutete ich, dass die Beeinträchtigung

der Navigationsfähigkeit durch das Ausschalten des RE auf die Wirkung auf die zielgerichteten Ortszellaktivierungssequenzen im Hippocampus zurückzuführen sein könnte. Um diese Hypothese zu testen, zeichnete ich die Aktivität von Neuronen im CA1 des Hippocampus auf und untersuchte ihre repräsentativen Positionen vor Beginn eines zielgerichteten Pfades mit und ohne Inaktivierung des RE. Während das Tier das Labyrinth erkundete, konnte ich keinen signifikanten Unterschied in der räumlichen Koordination der Ortszellen feststellen, so dass ich die Position des Tieres unabhängig von der Aktivität der RE-Neuronen genau dekodieren konnte. Ich beobachtete zielgerichtete Ortszellaktivierungssequenzen, bevor das Tier seine zielgerichtete Route an der eingefügten Wand vorbei begann, obwohl das Tier die Wand von seiner Startposition aus nicht sehen konnte, was darauf hindeutet, dass diese Aktivität die Planung einer Route um die Wand herum in der Dunkelheit unterstützen könnte. Ich untersuchte auch, ob sich die Eigenschaften der Ortszellaktivierungssequenzen im Hippocampus in Abhängigkeit von den Verhaltensanforderungen der Aufgabe ändern. Ich unterteilte alle Ereignisse in zwei Kategorien, Futtersuche und Zielsuche, basierend auf dem Zeitpunkt, an dem die Tiere ihre Verhaltensstrategie von zufälliger Suche (Futtersuche) auf zielgerichtete Navigation (Zielsuche) umstellen mussten. Dieser Unterschied verringerte sich jedoch während der Laser-On-Sitzungen. Diese Ergebnisse deuten darauf hin, dass die RE-Aktivität wahrscheinlich für neuronale Gruppen im Hippocampus entscheidend ist, um die Eigenschaften der Ortszellaktivierungssequenzen entsprechend den Navigationsanforderungen der Aufgabe zu verändern. Ich fand auch heraus, dass dieser Effekt auf die Zellaktivierung unabhängig

davon beobachtet wurde, ob die Wege von den geschlossenen oder den offenen Bereichen aus begannen.

Zusammenfassung und Ausblick

Ein zentrales Ergebnis dieser Dissertation ist, dass die Inaktivierung des RE zu einer Beeinträchtigung des Navigationsverhaltens und der zielgerichteten sequentiellen Aktivierung der Ortszellen führt, wie sie durch die Aktivität neuronaler Gruppen im Hippocampus CA1 repräsentiert werden. Die Korrelation zwischen der Beeinträchtigung der Routenplanung und der Abnahme von zielgerichteten Ortszellaktivierungssequenzen deutet darauf hin, dass die RE-Projektion für die Rolle des hippocampalen CA1 bei der Routenplanung notwendig ist. Insgesamt deuten meine Ergebnisse darauf hin, dass die PFC-RE-CA1-Schaltkreise eine entscheidende Rolle bei der Planung von Navigationsrouten spielen. Während in der Dissertation die verhaltensrelevanten und funktionellen Auswirkungen der Projektionen vom RE in den CA1 des Hippocampus untersucht wurden, ist noch unklar, wie genau die Aktivität der RE-Neurone die Eigenschaften der Ortszellaktivierungssequenzen im Hippocampus beeinflussen kann. Um dieser Frage nachzugehen, habe ich die Aktivität der RE-Neuronen mit einer Neuropixel-Sonde aufgezeichnet, während das Tier die gleiche Aufgabe ausführte. Eine weitere Analyse der RE-Aufzeichnungen könnte klären, wie die Aktivität der RE-Neuronen die zielgerichteten Ortszellaktivierungssequenzen im Hippocampus beeinflussen kann.

Chapter 1

Introduction

1. 1. Spatial navigation and its strategies

The successful implementation of goal-directed spatial navigation requires multistep computations – the estimation of one self's position and future destination, and the planning of corresponding journeys linking them. Despite this complexity, navigation ability is essential for all animals living in space, supporting their survival and reproduction. For example, animals are required to navigate to a nutrition source in the environment while avoiding plausible dangers along the path, to find an appropriate mate for reproduction, and to raise their offspring in a safe place. During the evolutionary process of animal species, there must thus be a selection bias for animals with better navigation ability.

Animal species have developed various navigation strategies that fit with their lifestyles. A primitive animal widely studied in biology, *Escherichia coli* (E. coli), uses a navigation strategy called chemotaxis, whereby an animal navigates along the concentration gradient of a particular chemical (Adler, 1966). This navigation strategy is observed universally

across many animal species, but it works only when a destination is close enough so that a diffused chemical from the source can be detected at the starting point of navigation.

What could be a navigation strategy that works in a broader range of space, such as ocean, desert, or sky? Green sea turtles (*Chelonia mydas*) are known for seasonal migrations over thousands of kilometers in the ocean. Several studies have suggested that these sea turtles can return to their home beaches by sensing the Earth's magnetic field (Avens & Lohmann, 2004; Lohmann et al., 2004).

Even a small insect has an amazing navigation ability. The desert ant (*Cataglyphis fortis*) lives in a desert without reliable landmarks in the environment. However, after traveling a long distance to search for food, ants can still return to their nest locations by taking a straight path, suggesting that they can maintain an accurate estimate of the direction and distance of the nest location during a journey (Müller & Wehner, 1988). Their navigation ability is known to be supported by a mechanism called "path integration", in which instantaneous movement direction and distance are accumulated during a journey, forming a homing vector indicating the direction and distance of the nest location (M.-L. Mittelstaedt & H. Mittelstaedt, 1980). The same navigation strategy is also described in other species, including rodents.

The navigation strategies described so far rely on either external sensory signals (e.g. magnetic field) or self's motions (e.g. path integration). Although these strategies work in an open space, our living environment is

often more complicated with boundaries, edges, and objects, such as buildings, trees, rivers, and roads. In such an environment, accurate estimates of the direction and distance of a destination are not sufficient because navigational planning should take into account the avoidance of these obstacles. This ability requires mapping of a spatial layout of the environment, such as boundaries, edges and objects. The behavioral psychologist Edward Tolman suggested that several animal species, including rodents and humans, can perform such mapping for navigation, possessing an internal map in the brain – a so-called cognitive map (Tolman, 1948).

The Tolman's cognitive map hypothesis is now widely accepted by the discoveries of place cells in the hippocampus (O'Keefe, 1976) and grid cells in the entorhinal cortex (Hafting et al., 2005). These neurons fire whenever an animal visits a particular location in space, which helps an animal to identify its own position in space. However, identifying the self's position is not sufficient for navigation. Navigational planning also requires estimating remote positions, such as goals and routes, but it is still largely unclear whether and how this cognitive map can be used to locate positions away from the self. Given that a recent study identified the orbitofrontal cortex as a goal map (Basu et al., 2021), my particular interest here is how an animal can plan a navigational route that avoids known but unseen obstacles in the environment. This dissertation aims to clarify its underlying neural mechanisms by identifying key brain regions and deciphering their neural codes for navigational route planning.

1. 2. Neural circuits for route planning

The hippocampus is thought to play a pivotal role in supporting our higher cognitive abilities, including episodic, semantic, and spatial memory formation, as well as goal-directed navigation relying on a cognitive map. Previous studies suggest that neurons in the hippocampus represent information about an animal's future movements during navigation. When an animal approaches a T-junction of the maze, place cells in hippocampal CA1 show differential firing depending on the choice of the animal's next movement direction (Wood et al., 2000; Ito et al., 2015). Another study suggests that sequential firing among hippocampal neural ensembles before starting navigation can predict the animal's upcoming trajectories (Pfeiffer & Foster, 2013). These studies suggest that hippocampal neurons encode information about the animal's next movement direction, which may support the ability for route planning.

However, the existence of information in a particular brain region does not necessarily mean that this information is generated there. For example, the differential firing of CA1 place cells before the T-junction has been shown to be dependent on inputs from the prefrontal cortex (PFC) (Ito et al., 2015). Ito et al. found that trajectory-dependent firing is observed across the medial PFC, the hippocampal CA1, as well as the nucleus reuniens of the thalamus (RE) – an anatomical hub between the PFC and hippocampal CA1. Inactivation or lesioning of the RE disrupted differential firing in CA1, suggesting that future movement information is transferred from the medial PFC to CA1 via the RE.

The key roles of the PFC in navigation have been demonstrated in several previous studies. For example, a patient with damaged PFC showed a problem in goal-directed navigation (Ciaramelli, 2008). However, when this patient was reminded of the goal location during navigation, he was able to navigate correctly. This suggests that the PFC is likely essential to maintain information about navigational goals. In support of this idea, a recent study reported that the rat orbitofrontal cortex (OFC), a subregion of the PFC, serves as a goal map for navigation, persistently pointing to the animal's next target destination during the journey (Basu et al., 2021).

While both the PFC and the hippocampus are considered essential brain regions for navigation, there are essentially no direct anatomical connections from the PFC to hippocampal CA1. That is why the RE is thought to play a key role here. Multiple studies have confirmed reciprocal connections between the PFC (medial PFC and OFC) and the RE, by using either retrograde tracers (Herkenham, 1978; McKenna&Vertes, 2004) or anterograde tracers (Herkenham, 1978; Vertes, 2002; Vertes et al., 2022). The RE also gives rise to excitatory inputs in CA1 but not in CA3 or the dentate gyrus (Wouterlood et al., 1990; Dolleman-van der Weel & Witter, 1996).

The expression level of the immediate early gene c-Fos has been shown to increase in the RE during the Morris water maze task, supporting the involvement of the RE in navigation (Loureiro et al., 2012). However, neurotoxic lesions of the RE did not affect either the animals' navigation or memory performance in the water maze task (Dolleman-van der Weel et al., 2009; Ghiafeh et al., 2009), raising the question of the role of the RE in

navigation. However, these studies did not consider a plausible role of the RE in route planning, because all the behavioral tests were performed in an open maze without obstacles. One of the main aims of this dissertation is thus to investigate the role of the RE in navigational route planning by designing and performing a new navigational task.

1. 3. Aims of the dissertation

In a complex environment with multiple boundaries, edges, and obstacles, the ability for navigational route planning is particularly important for an animal's survival. Previous studies have suggested the dedicated roles of the hippocampus and the PFC in representing the animal's own position and its destination, respectively. I thus hypothesized that the interactions between the PFC and the hippocampus are the key to deciphering the navigation circuits in the brain. My dissertation aims to test this hypothesis with the following three objectives.

1. Clarify the role of RE in the ability for route planning by optogenetically inactivating RE neurons -*Chapter 3*

2. Determine the role of the hippocampus in route planning by chemogenetically inactivating hippocampal neurons -*Chapter 4*

3. Deciphering neural codes supporting route planning in the hippocampus and clarifying the impact of RE neurons. -*Chapter 5*

Chapter 2

Materials and Methods

2. 1. Subjects

Four male Long-Evans rats (335, 509, 391, and 451) were 3~6 months old at the start of the experiment. All animals were housed individually in Plexiglass cages (45 x 35 x 40 cm; Tecniplast, GR1800) in the animal facility under a reverse light-dark cycle (light phase, 10:00 PM to 10:00 AM) at least from three days before the start of the experiment. All animal experiments were performed during the dark phase of the cycle. Animals had ad libitum access to food and water except when they were in deprivation for the behavioral task.

Rat 335 and 509 received adeno-associated virus (AAV) injections and optical fiber implantation in the RE for optogenetic silencing experiments and tetrode drive implantation to record bilateral hippocampal CA1 neural signal recordings. Rat 391 underwent AAV injections and optical fiber implantation for optogenetic silencing experiments and Neuropixel probe implantation to verify the manipulation of the neuronal population in the RE. Rat 451 received bilateral hippocampal AAV injections for Designer

Receptors Exclusively Activated by Designer Drugs (DREADDs) experiments, and a 3D-printed LED holder was fixed to the skull with dental cement and anchor screws to hold LEDs for position tracking in hippocampal inactivation experiments.

All animal procedures were approved by the local authorities (Regierungspräsidium Darmstadt, protocols F126/1009, F126/1026, and F126/2005) in accordance with the European Convention for the Protection of Vertebrate Animals used for Experimental and Other Scientific Purposes.

2. 2. Surgery, virus injection, and drive implantation

The rats were anesthetized in the induction chamber with isoflurane initially at a 5.0% concentration. The isoflurane concentration was then adjusted according to the physiological monitoring of the rats and maintained between 0.5-3% (v/v) during surgery. For analgesia, buprenorphine (Bupresol, 0.06 mg/ml, CP-Pharma) was induced by subcutaneous injection followed by local intradermal injection of either bupivacain (Bupivacain 0.25% (w/v), Jenapharm) or ropivacain (Ropivacaine Hydrochloride, 2 mg/ml, Fresenius Kabi) into the scalp. Subsequently, the animal was fixed in a Kopf stereotaxic frame and placed on a warm pad to maintain body temperature above 35°C throughout the surgery. An eye cream (Bepanthen eye cream, Bayer) was applied to prevent eye dryness. After the surgery, all animals received the analgesics meloxicam orally (Melosus 1.5 mg/ml, CP-Pharma) or by subcutaneous injection (Metacam, 2 mg/ml, Boehringer Ingelheim) for at least 3 days postsurgery.

For the optogenetic manipulation experiments (Figure 3. 1A), a solution of AAV was injected into the RE unilaterally or bilaterally using a 10-μl syringe (Nanofil syringe, World Precision Instruments) with a 33-gauge needle (Nanofil 33G BVLD needle, World Precision Instruments) at four sites (AP: -2.2 and -2.7, ML: as close as possible to the midline, DV: 6.6 and 7 in mm from the bregma, with a 7.5° lateral-to-medial angle to target the relative midline of the RE). The injection volume (0.4 μl at each site) and flow rate (0.1 μl/min) were controlled by a Micro4 microsyringe pump controller. After the injection, the needle remained in the same place for 10 minutes and was then withdrawn slowly. An optical fiber was subsequently implanted in the RE (AP: -2.4, ML: as close as possible to the midline, DV: 6.5, with 7° lateral to medial angle). A Neuropixel probe was then implanted in the RE (AP: -2.25, ML: as close as possible to the midline, DV: 7.5, with 6° lateral to medial angle) from the other side of the hemisphere to monitor neuronal activity and manipulation by optogenetic methods.

To verify the impact of RE silencing on the activity of hippocampal CA1 neurons (Figure 4. 1A), a microdrive with 28 individually adjustable tetrodes was implanted into the bilateral hippocampus. The tetrodes were implanted on the surface of the cortex above the dorsal hippocampus (AP: -4, ML: ±3.5) with or without an angle of 10° toward the anterior direction. The tetrodes drive was secured on the skull with screws and dental cement. Two screws above the cerebellum were connected to the ground of the tetrode drive.

2. 3. Electrode turning and recording procedures

A tetrode microdrive holder was printed with the 3D printer. Tetrodes were made from 17 um polyimide coated platinum-iridium wire (90%-10%; California Fine Wire Company) and plated with gold to reduce the impedances below 150 kOhm at 1004 Hz. The tetrode insertion in the bilateral hippocampus was guided by two circular bundles (made of 30-gauge stainless steel tubing), each of which can hold 14 tetrodes. Tetrodes were implanted on the surface of the brain initially and lowered down to 0.75 mm after being fixed during the surgery. One tetrode from each hemisphere was used as a reference electrode in the superficial layers of the cortex (DV: ~1 mm from bregma). Other tetrodes were lowered daily toward the pyramidal layer of the hippocampus by monitoring LFP and spike activity. The tetrode movement was stopped one day before recording experiments to maintain stable recordings.

2. 4. Behavior task

The behavioral task was designed based on a task used by Pfeiffer and Foster (2013). In this task, rats are required to alternate between random searching (random-well-searching trial) and goal-targeting (home-targeting trial) in a two-dimensional environment. This allows us to compare two different behavior types in the same environment with the same recording condition. At the beginning of the experiment, a home well was filled with a

water reward. The rat was then introduced in the maze and was required to find the home well to initiate the main task program.

Our task design is different in several aspects from the one used in Pfeiffer and Foster (2013). First, a water reward was delivered only after the animal licks a correct well for a specified time threshold (300 ms), which improved the animal's understanding of the task rule and helped it target the home well directly. Second, an L-shaped wall was introduced in the arena. This modification allows us to examine not only an animal's goal-directed behavior, but also its ability to plan a wall-avoiding route. Finally, all experiments were performed under minimum light conditions. All the lights were turned off and the maze was surrounded by black curtains, which forced an animal to plan goal-directed behavior based on the brain's cognitive map without relying on visual identification of landmarks.

2. 4. 1. Apparatus design

The maze is a 1.5 m x 1.5 m square shape with a black floor and walls. Twenty-five water delivery wells of the same shape were evenly distributed on the floor. The maze floor was raised from the experiment room floor to have space for all wires connecting to the infrared sensors for lick detection and the tubings for delivering a water reward to individual wells. A reward solution contained 0.03% saccharin and was stored in a sealed bottle outside the maze. Peristaltic pumps delivered a precise amount of a water reward. A black acryl L-shaped wall was placed in the center of the maze arena. The wall has 60 cm x 90 cm edge lengths with 25 cm height (Figure 3. 3A). A

black curtain with no external cues surrounded the apparatus, and all lights in the experimental room were turned off. Four loudspeakers were placed on the ceiling at each corner of the maze to deliver the sound cue and white noise.

2. 4. 2. Water restriction

Animals' water consumption was restricted to motivate water-seeking behavior in the task. The animals' daily weights and water consumption were monitored during habituation days. The restriction was started from the end of habituation days, and animals consumed 20% of the original consumption volume.

2. 4. 3. Handling, habituation, and pretraining

Animal handling and maze-habituation were performed without water restriction. Handling was performed for 5 consecutive days (3 days in the animal facility and 2 days in the experimental room) before starting behavioral experiments. After handling, the animals were placed in the maze and habituated to the environment for 2 days without water restriction. During habituation, black plastic barriers of the same height were placed to restrict the animal's access only to an area with four water-delivery wells. Four wells were prefilled with water before the animal was placed in the maze. When the animal's licking was detected by an infrared sensor at a well, a water reward was further delivered in this well together with a beep sound cue (2000 Hz, 200 ms).

After the habituation, the animals went under water restriction. Pretraining was composed of 3 phases, by increasing the number of accessible wells from 4 wells, 10 wells, to 25 wells. Black plastic barriers prevented the rat's access to unused wells in each task phase. During this pretraining phase, the animals learned the existence of two trial types in a behavioral session – random-well-searching and home-targeting trials. Home-targeting trials were defined as 'correct' when the animals navigated to the home well directly from a start position without licking other wells along the path. The animals were trained until the percentage of correct trials exceeded 80%.

2. 4. 4. Behavior test

After surgery, the animals were allowed to recover without water restriction for at least 5 days. The animals were then re-trained on the behavioral task under water restriction. Three 15~20 minute behavioral sessions were performed each day. When the correct percentage reached 80%, the home well was changed to a new location, and the animal's position and neuronal activity were recorded. Once the correct percentage reached 80% for the new home, an L-shaped wall was introduced in the maze arena. The impact of the wall on the animal's behaviors was assessed for the first 3 days following wall introduction. The animals were then trained until the correct percentage reached 80% in the maze with the inserted wall.

For the optogenetic RE inactivation experiment, the comparison was performed between sessions (Figure 3. 1D). The first two sessions were used

for the control session. After the second control session, the 470 nm laser pulses (150 ms, 0.1 Hz) started and were maintained during the entire laser-on behavioral sessions. After the end of the laser-on session, the 470 nm laser application was stopped, and the 630 nm laser was applied for 3 seconds to inactivate SwiChR++ channels, helping to restore RE neuron activity. The recovery session was then started and continued as long as the animal maintained sufficient motivation to the task.

For the pharmacogenetic hippocampus inactivation experiments, the animal's behavioral performances were compared between daily sessions either with or without inactivation (Figure 4. 1D). Water (Aqua, Braun) was subcutaneously injected on the control days, whereas the DREADDs agonist deschloroclozapine (DCZ) was injected on the test days. The behavioral sessions started one hour after the injection. No solution was injected on the recovery days.

2. 5. Histology

After the completion of the experiments, the rats were anesthetized with isoflurane and received pentobarbital by intraperitoneal injection. Intracardial perfusion was performed initially with saline, followed by a fixative solution of 10% formalin. The brain was extracted and stored in formalin solution for at least 72 hours at 4°C. To visualize the virus expression of SwiChR++-YFP, 40 μm coronal brain sections were collected in TBS solution, which were then stained with DAPI (Hoechst 33342, Invitrogen) as well as an antibody against YFP. For optical fiber and

electrode traces, 30~40 μm coronal sections were mounted on slide glasses and stained with cresyl violet. To confirm the expression of hM4Di-mCherry for the DREADDs experiments, fluorescent imaging using a serial block-face scanning microscope was performed for the entire brain to construct a 3D fluorescence image.

2. 6. Data analysis

2. 6. 1. Behavior analysis

All data processing and analysis was performed in MATLAB (Mathworks). The animals' position was sampled with 25 Hz using two-colored LEDs attached to the recording headstage. Timestamps of the infrared sensor interruptions by the animal's licking behaviors as well as the times of reward delivery were recorded.

Among all home-targeting trials in a behavioral session, those with the animal's licking at a well other than the home were considered error trials. The error rate was calculated at individual start wells. The change in error rates was monitored for the first three days following wall introduction. The error rate was the number of error trials divided by the total number of trials over 3 days.

For the comparison of the animal's goal-targeting behavior paths between sessions (e.g. control vs laser-on), only correct trials were considered. The beginning of goal-targeting behavior paths was defined based on the time when the animal's running speed exceeded 10 cm/s and its

position was at least 10 cm away from the start well. Because the animal's start positions were different in individual home-targeted trials, the path lengths and the time durations of trials were normalized (z-scored) for the same start-home well pairs across sessions. The animal's movement direction was defined as the angle between the animal's present position and the one at 100 ms ahead. The variance of the movement direction was calculated for 20 consecutive values of the movement direction.

2. 6. 2. Spike sorting

Neural signals were acquired and amplified by two 64-channel RHD2164 headstages (Intan Technologies) using an OpenEphys acquisition system, sampled at 15 kHz. The recorded signals were bandpass filtered at 0.6~6 kHz for spike detection. The Kilosort program was used to isolate individual spikes and assign them to separate clusters based on spike-waveform characteristics across channels (https://github.com/cortex-lab/KiloSort) (Pachitariu et al., 2016).

2. 6. 3. Spatial correlation and place cell classification

The spike position data of each session type within each recording day were divided into 10 equally sized bins. Two spatial firing rate maps were generated based on odd or even bins of spike position data in each session type. If the spatial correlation of the two spatial rate maps was greater than 0.6, the cell was classified as a place cell. The spatial correlation between

control and laser-on sessions was calculated using the spatial rate map from the entire data of each session type.

2. 6. 4. Decoding analysis

The spike activity of each neuron was smoothed (Gaussian kernel, sigma 250 ms). Mean firing rates of a neuron at individual position bins of the size of 2.5 cm x 2.5 cm were computed when the animal's running speed exceeded 5 cm/sec (Figure 5. 2).

A Bayesian decoder was constructed to estimate the animal's position based on the activity of a neural population (e.g., Pfeiffer and Foster, 2013). The probability of the animals' position (pos) across total position bins (M) with the neural spikes (spikes) in a time window (τ) is

$$Pr(pos|spikes) = \cup / \sum_{j=1}^{M} \cup$$

where

$$\cup = \left(\prod_{i=1}^{N} f_i(pos)^{n_i} \right) e^{-\tau \sum_{i=1}^{N} f_i(pos)}$$

Here, $f_i(pos)$ is a spatial tuning curve of the i-th unit. I used a uniform prior over the positions and assumed Poisson firing statistics for all N units. The animal's positions were estimated at individual 250 ms bins across a session.

2. 6. 5. Trajectory sequence analysis

Sequential firing of a neural population representing a navigational trajectory was assessed during well licking - from the time when the animal initiated licking a particular well until it stopped licking and left the well. I further restricted this duration to the animal's running speed below 10 cm/s. The Bayesian decoder constructed based on the animal's exploratory behavior was applied to the neural population activity during the time of well licking. A position was estimated at individual 20 ms time windows with a 5 ms increment. A series of decoded positions was considered a trajectory event when a position sequence longer than 30 ms satisfied the following conditions: 1) the distance between consecutive positions was within 20 cm apart, and 2) the sequence went beyond 25 cm away from the animal's position.

During random-well-searching trials in the task, the animal could not tell whether a licking well was the correct one or not until it heard a beep sound with water delivery. I also set a time threshold of 300 ms for which the animal was required to keep licking a well before sound generation. These task settings imply that a beep sound may elicit a change in the animal's navigational intention from random-well-searching to goal-targeting navigation. I thus categorized the licking time and associated trajectory events before and after a beep sound. One category is trajectory events generated during the random-well-searching phase, including the time before a beep sound at the correct random well (foraging-phase events). Another category is those generated after the beep sound at the correct random well (homing-phase events). Note that foraging-phase events include those

generated while the animal licked multiple wells during the random-well-searching, whereas homing-phase events include only the ones at the correct random well.

To visualize the animal's paths and the trajectory events, the positions were normalized so that the animal's position and the home-well (goal) position were aligned in the same line. A binomial test was performed to compare the densities of trajectory events at the goal and the animal's position. The ratio of the trajectory density at the start and the goal was compared between the foraging and the homing phase events.

2. 7. Statistical procedures

All statistical tests were nonparametric tests. Error bars in all figures represent the standard error of the mean (SEM). All box plots show median $\pm$ SEM.

Chapter 3

The Role of the Nucleus Reuniens in Planning an Obstacle-avoiding Route to a Remembered Goal

3. 1. Introduction

The nucleus reuniens (RE) is a ventral midline thalamic nucleus that serves as an anatomical hub between the prefrontal cortex (PFC) and the hippocampus (Vertes et al., 2007; Cassel et al., 2013). The RE has attracted more attention lately because of several recent studies suggesting a key role of prefrontal-hippocampal interactions in spatial navigation. However, these previous studies investigated the RE's function using a relatively simple navigation task in which an animal was forced to run along a narrow track without flexible choices of movement directions (Cholvin et al., 2013; Layfield et al., 2015; Viena et al., 2018), which might have prevented from understanding the RE's role in a broader perspective.

Here, I investigated the RE's role by designing and implementing a new goal-directed navigation task. The task was specifically designed to test the rats' ability to plan an efficient route to a destination in a familiar environment with obstacles. All experiments were performed in darkness, forcing an animal to rely on a cognitive map, rather than sensory perception

of landmarks. The animals were trained to navigate to a fixed goal location from various starting positions, allowing us to test the animal's ability for flexible route planning. To test the causal role of the RE, I applied an optogenetic method to silence the activity of RE neurons during goal-targeting journeys, and examined its impact on the animal's ability to take an obstacle-avoiding route to a given destination.

3. 2. Results

3. 2. 1. RE inactivation did not impair goal-directed behavior in an open arena

I injected an adeno-associated virus (AAV) encoding SwiChR++ and eYFP under the CaMKII-promoter in the RE. SwiChR++ is a chloride channel opsin that can be activated by blue light (473 nm wavelength) and deactivated by red light (635 nm wavelength) (Berndt et al., 2016). An optical fiber was implanted in the RE to apply laser light to neurons expressing SwiChR++ (Figure 3. 1A).

A Neuropixel probe was further implanted in the RE of one animal (Rat 391) following the AAV injection and optical fiber implantation in the RE, to examine the impact of laser application on the spiking activity of SwiChR++-expressing neurons. I found that a 150 ms pulse of blue laser (470 nm) reliably decreased the spiking activity of a subset of recorded neurons (Figure 3. 1B). I also confirmed that these inactivated neurons recovered their

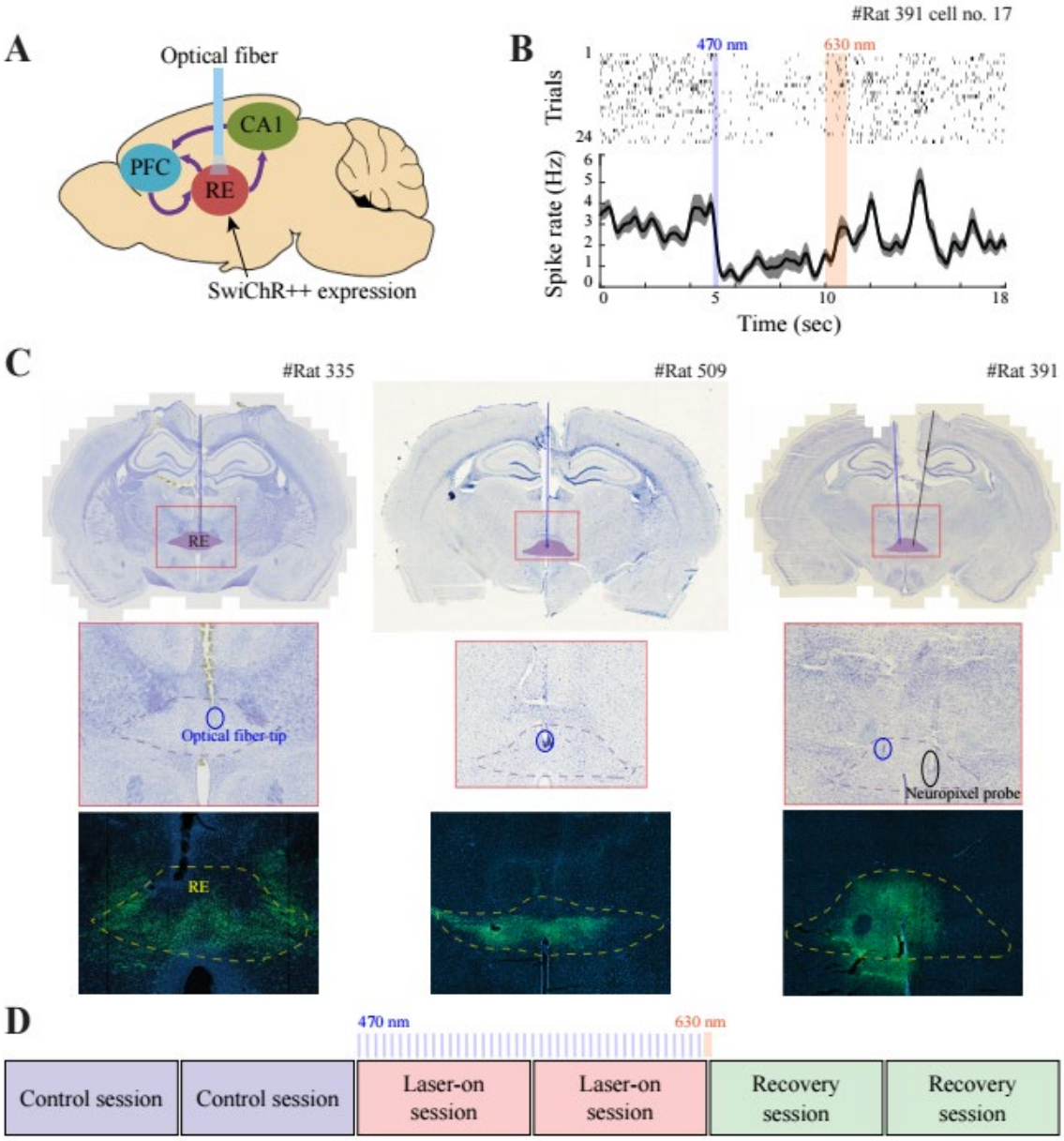

Figure 3. 1. Silenced neural activity in the RE using the optogenetic method

A) AAV-mediated expression of CamKII-SwiChR++-eYFP in the RE to silence the activity of RE neurons, enabling to perturb information transfer from the PFC to CA1. An optical fiber was implanted in the RE where the virus was injected. **B)** Spike rates of a representative RE neuron in response to the laser application. Color rectangles indicate laser-applied time points. In each trial, 470 nm wavelength blue laser was applied for 150 ms followed by 3 s of 635 nm wavelength orange laser application after 5 s at the end of the blue laser. Mean and 95% confidence intervals (shaded) are shown. Raster plot of the total of 24 trials above. **C)** Coronal sections of the brain showing the RE. Upper low, cresyl violet stained coronal section showing

the optical fiber trace (blue line) and the Neuropixel probe trace (black line in rat 391) in the RE (purple shade). Middle low, higher magnification of the RE (purple dashed line) in the same section showing the tip of the optical fiber (blue circle) and the Neuropixel probe (black circle). Bottom, YFP-immunostained (green) section showing virus expression in the RE (yellow dashed line). **D)** Scheme of a daily schedule of behavior sessions for optogenetics experiments, composed of control, laser-on (RE inactivation), and recovery sessions. Usually, two sessions were conducted for each. Blue laser pulses were applied throughout the entire laser-on session, and orange laser was applied at the end of the laser-on session, before starting the recovery session.

spiking activity after 3 seconds of red laser (635 nm) application. The histological examination of the brain sections for eYFP expression and optical fiber tracks further confirmed the successful optogenetic targeting of RE neurons (Figure 3. 1C).

I tested the animal's navigation ability by performing 6 behavioral sessions per day. The duration of each session was 15 to 20 minutes. Typically, the animals with sufficient training were able to perform more than ten home-targeting trials in each session. A daily experiment started with two behavioral sessions without manipulation ('control'). The animal subsequently performed the two sessions under the application of blue laser pulses (150 ms, 0.1 Hz) during the entire duration of the sessions ('laser-on') to inactivate RE neurons. Once the animal completed the RE-inactivation sessions, a 5-second red laser pulse was applied before starting the subsequent session so that RE neurons recovered their activity. Finally, the animal performed two additional behavioral sessions ('recovery') (Figure 3. 1D).

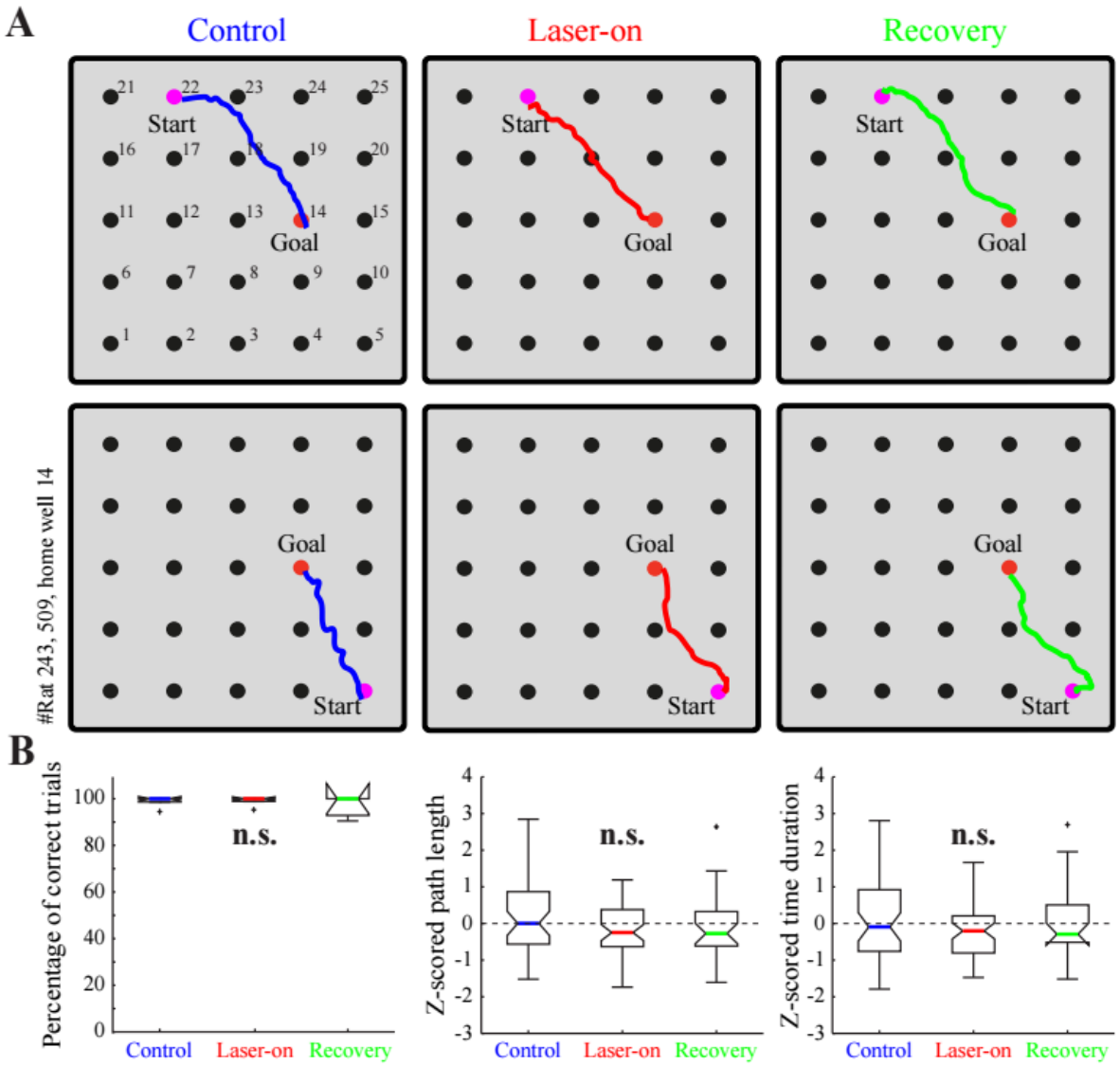

Figure 3. 2. RE inactivation did not impair the animal's ability for goal-directed navigation in an open-field arena

A) Two examples of an animal's behavior paths in the home-targeted trials. The top-left maze scheme indicates the well numbers (1-25). The example behavior paths are from two start locations (top, well no. 22; bottom, well no. 5) to the same home location (well no. 14), showing control (left, blue), laser-on (middle, red), and recovery (right, green) trials, respectively. The animals did not show any apparent change in goal-directed behaviors under the silencing of RE. **B)** Left, a plot shows the percentage of correct trials, indicating no statistical difference between session types ($p = 0.79$ in Kruskal-Wallis test). Each dot indicates a value from each session. Middle and right, plots show either path length or time duration (z-scored) of behavior

paths on the home-targeted trials. No statistical difference was observed between sessions (path length: $p = 0.44$ in Kruskal-Wallis test; time duration: $p = 0.55$).

The animals were initially trained in a goal-directed navigation task in an open-field arena –the same maze setting (see Methods) as in the study by Pfeiffer and Foster (2013). The maze has 25 equidistantly distributed wells (Figure 3. 2A, top-left), each of which can detect an animals' licking by an infrared sensor and deliver a water reward when the licked well is the correct one.

I found that the silencing of the RE neurons did not cause any significant behavioral deficit in the task (Figure 3. 2A). No statistical difference was observed between control and RE-inactivated sessions in the animal's task performance [the number of correct trials / the total trial number × 100] ($p = 0.79$ in Kruskal-Wallis test), the z-scored path length ($p = 0.44$ in Kruskal-Wallis One-way ANOVA test) and journey duration ($p = 0.55$ in Kruskal-Wallis test) of the animal's goal-targeting paths (Figure 3. 2B). In fact, this result was consistent with the previous study in which the authors did not find any impairment by RE lesioning in the animal's ability to perform for the Morris water maze task (Dolleman-van der Weel et al., 2009), suggesting the RE is dispensable for goal-directed navigation in an open field arena.

3. 2. 2. Modified task design induced two different navigation strategies

The absence of the impact of the RE silencing on the animal's performance led me to the possibility that this behavioral task may not be ideal for dissecting the functional role of the RE. The major caveat of this task design is that the successful performance does not require the ability for route planning. For example, in both the Morris water maze task and the Foster task, an animal can take a straight path to a given destination, without the need to avoid obstacles in the environment. To test this possibility, I introduced a wall in the open-field arena and let animals perform the same Foster task (Figure 3. 3A). This modified task will thus require an animal not only to reach a destination, but also to avoid the wall during a goal-targeting journey. Here, the choice of an L-shape wall allows us to test the animal's ability to choose an optimal route between two plausible ways to access the goal.

The introduced wall divides the animal's goal-targeting journeys into two conditions, either when a straight path to the goal is occluded by the wall or not. If a straight path is unavailable, the animal is required to plan a detour path to the goal by avoiding the wall. By contrast, when a straight goal-targeting path is available, the animal can simply take the same navigation strategy as in an open arena. The home well was changed after sufficient data collection to exclude a possibility for the animal to memorize all the possible routes. The start wells are classified according to the home-well choice (Figure 3. 3B, straight-path occluded in magenta and non-occluded in cyan).

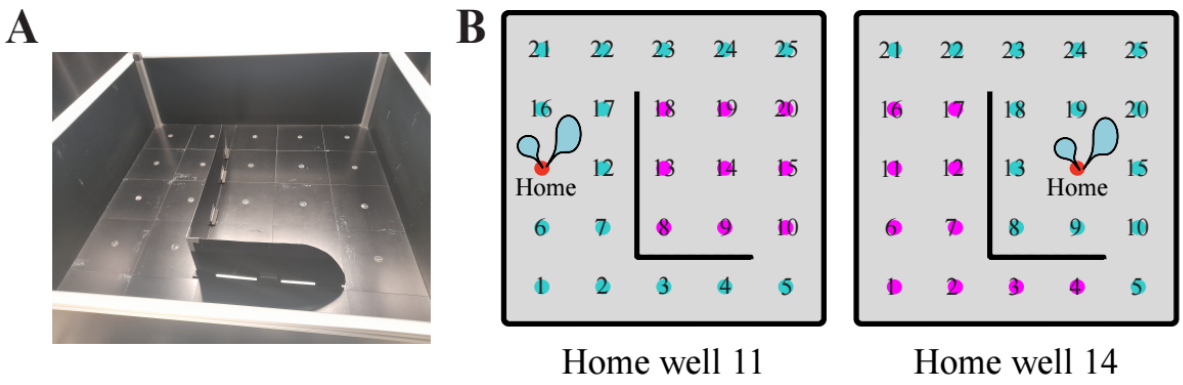

Figure 3. 3. An L-shaped wall introduced in the maze

A) Photo of the maze with an L-shaped wall inside. **B)** The wall divides the arena into two categories (cyan and magenta color) depending on the home location. The two home wells (no. 11 and 14) are marked in red color. The start wells from which a straight path to the home well is blocked by the inserted wall are categorized as 'occluded' (magenta), while those from which a straight path is available are 'non-occluded' (cyan).

The animal's behavior on the first few days after the wall introduction exhibited a contrasting difference in its performance between the two start-well categories (Figure 3. 4). When the animal started from positions where a direct goal-targeting path was available, I did not find any significant difference in its performance from that in the open maze ($p = 0.66$ in Kruskal-Wallis test, the performance was calculated for the first three days after the introduction of the wall, Figure 3. 4A). By contrast, when the animal started from positions from which a straight goal-targeting path was blocked by the wall, it showed apparent difficulty in finding the home location and licked incorrect wells before reaching the destination. Correspondingly, the performance dropped significantly ($p < 0.05$ in Kruskal-Wallis test) compared to that in the open maze. I also calculated the error rate difference

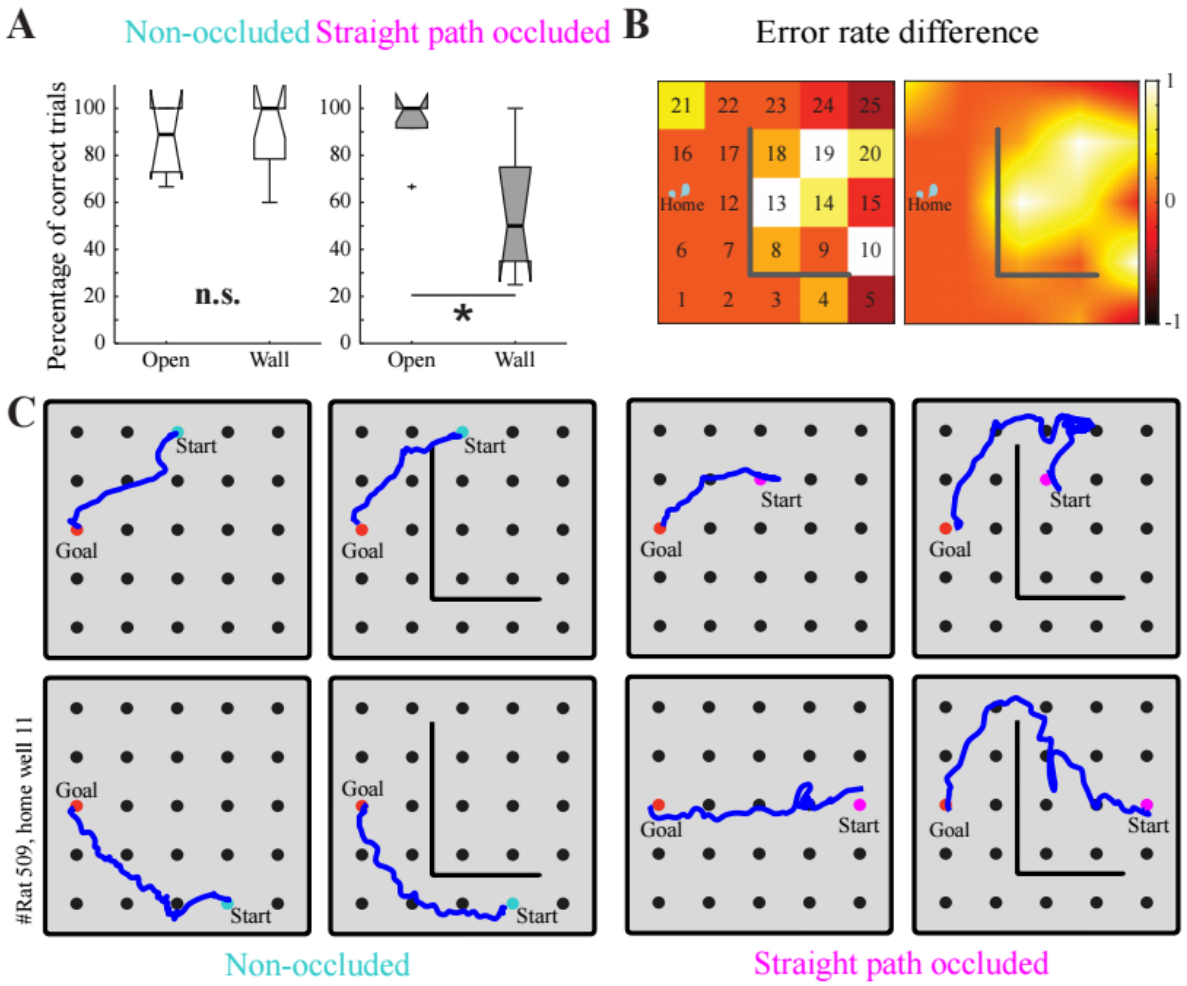

Figure 3. 4. Wall introduction impaired accurate goal targeting when a straight path to a goal was occluded

A) The correct performance after the wall introduction was not significantly changed from the one in the open-field maze when the animal started from the wells in a non-occluded zone ($p = 0.66$ in Kruskal-Wallis test), but was dropped significantly when it started from an occluded zone (right, $p < 0.05$ in Kruskal-Wallis test). **B)** Left, error-rate differences on individual wells before and after the wall introduction; right, same plot but smoothed. The gray lines indicate the position of the inserted wall. **C)** Examples of behavior path changes before and after the wall insertion, navigating between the same start-goal well pairs. Note non-smooth behavior paths particularly when the animal started from the occluded zone of the wall-inserted maze.

(see Methods) between before and after the wall introduction at individual start wells on the maze (Figure 3. 4B, the gray lines indicate the wall position), which demonstrated the overall increase of error rate from the start positions where a direct goal-targeting path was occluded by the inserted wall. Even on correct trials, the animal took wiggled-longer behavior paths until it escaped from the occluded zone (Figure 3. 4C, left). But such behavior was usually not observed when the animal started from the non-occluded zone (Figure 3. 4C, right).

However, after sufficient training in the wall-inserted maze (> 5 days), the increased error rate in the occluded zone disappeared, and the animal's task performance reached over 80%. I did not find any significant difference in the performance between before and after the wall insertion (non-occluded, $p = 0.75$; occluded, $p = 0.44$ in Kruskal-Wallis test), suggesting that the animals were able to recognize the home well correctly (Figure 3. 5C, top).

To assess the animal's strategic change in taking a smooth wall-avoiding path (Figure 3. 5A), I compared the lengths and durations of the animal's goal-targeting journeys before and after the wall insertion. To take into account the path differences due to different combinations of start and goal wells, I took z- scored values for individual start-goal well combinations. The averaged z-scores for the path length and time duration of goal-targeting paths are displayed at each well location in the maze (Figure 3. 5B). This plot shows that the z-scored values for the path length and time duration are overall larger in the occluded zone, indicating the change in the animal's paths for wall avoidance.

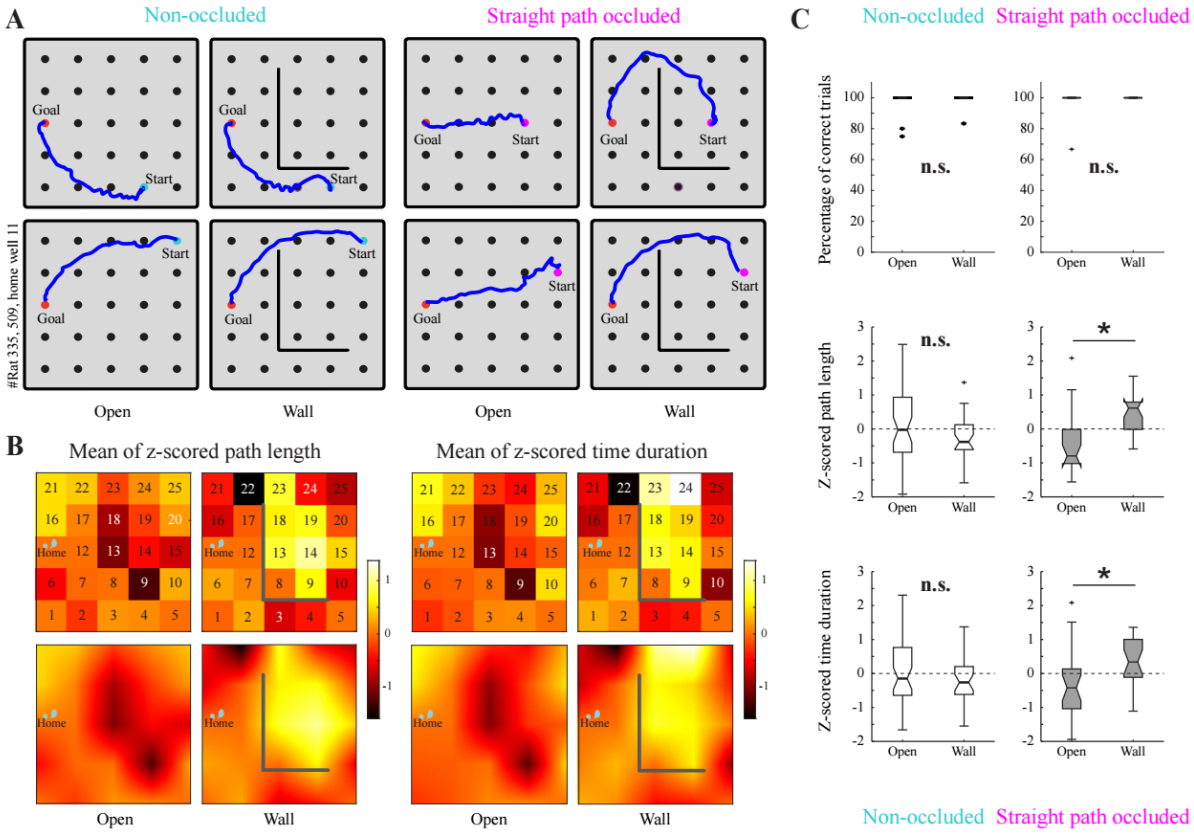

Figure 3. 5. Training improved the task performance where the animals learned to take a wall-avoiding path.

A) Example of an animal's behavior paths between the same start-goal pairs, either in the open field task or after sufficient training in the wall-inserted arena (> 5 days). Behavior paths started from the non-occluded (left) or occluded (right) zone are shown separately. **B)** Averages of z-scored path length (left) and time duration (right) are shown for each start well. The gray line indicates the position of the inserted wall. **C)** Top, plot shows the animal's task performance, which did not show any significant difference between the open-field and the wall-inserted mazes (non-occluded $p = 0.75$; occluded $p = 0.44$ in Kruskal-Wallis test). Middle and Bottom, plots show the z-scored path length and time duration of goal-targeting behavior paths, showing any significant differences in trials started from the non-occluded zone (path length $p = 0.18$; time duration $p = 0.34$ in Kruskal-Wallis test), whereas significant differences were observed in those started from the occluded zone ($p < 0.05$ in Kruskal-Wallis test).

When comparing the z-scored path lengths and time durations of goal-targeting paths before and after the wall insertion, I did not find any difference in the trials started from the non-occluded zone (path length, $p = 0.18$; time duration, $p = 0.34$ in Kruskal-Wallis test), but significant increases were observed on the trials started from the occluded zone ($p < 0.05$ in Kruskal-Wallis test).

These results together suggest that rats can plan and take an efficient navigation route to avoid known obstacles to reach a desired destination. Importantly, I conducted these experiments in a minimum light condition so that animals were unable to identify the wall location visually at the start position, and thus these results suggest that the rat has the ability to plan an obstacle-avoiding route by relying on the brain's internal model of space – the cognitive map.

3. 2. 3. RE silencing impaired goal-directed behavior when the straight path is occluded by the wall

To test the role of the RE in the animal's ability to plan a wall-avoiding route, I conducted optogenetic silencing of the activity of RE neurons while the animals performed the navigation task in the wall-inserted maze. The experimental design (order, number, and length of sessions per day) was the same as that for optogenetic experiments in the open field arena (section 3. 2. 1).

During the RE silencing, the task performance did not change significantly during the laser-on session in both the non-occluded and the

occluded condition (non-occluded: $p = 0.84$; occluded: $p = 0.81$ in Kruskal-Wallis test) or between the non-occluded and the occluded conditions ($p = 0.15$ in Kruskal-Wallis test) (Figure 3. 6A), indicating that the animals maintain the ability to identify the correct home location. To assess the impact of the RE inactivation on the animal's general movement ability, I calculated the maximum running speed during random-well searching behavior, and found that it did not change significantly across the session types either in the non-occluded condition ($p = 0.31$ in Kruskal-Wallis test, Figure 3. 6B, left), the occluded condition ($p = 0.38$, Figure 3. 6B, right), or between the non-occluded and the occluded conditions ($p = 0.50$ in Kruskal-Wallis test), suggesting that the animal's movement ability was intact during RE inactivation.

I analyzed all the correct goal-targeting journeys and compared them between the control, laser-on, and recovery conditions (Figure 3. 6C). To analyze the smoothness of the animal's paths, I calculated the variance of movement directions in a time-resolved manner along the journey by using moving time windows (see Methods; Figure 3. 6D). The journey times were normalized across trials. I did not find any impact of RE silencing on the movement variance when the animals started from wells in the non-occluded zone ($p = 0.06$ in Friedman's test). By contrast, I found that the RE silencing significantly increased the movement variance when the journeys started from the occluded zone ($p < 0.05$ in Friedman's test).

I further tested the impact of RE inactivation on the path length and the time duration of goal-targeting journeys. Again, the path length and the time duration were z-scored across trials with the same pairs of start and goal wells.

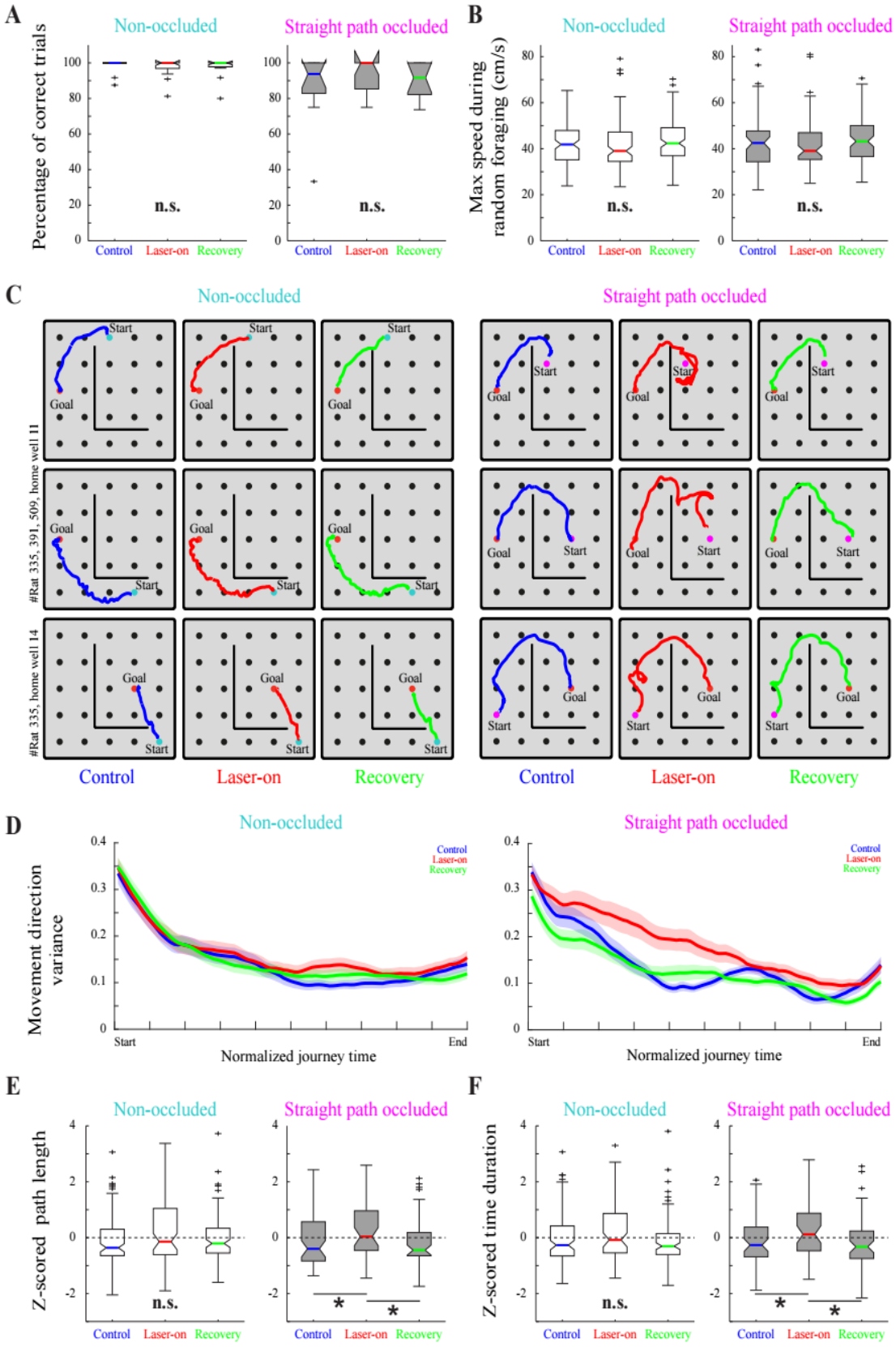

Figure 3. 6. RE silencing caused the rats to take a non-smooth longer path when a straight path to the goal was occluded by the inserted wall.

A) Plots show the task performance. Each dot indicates the percentage of correct trials in each session. Kruskal-Wallis test showed no significance between session types irrespective of trials started from the non-occluded zone (left, $p = 0.84$) or the occluded zone (right, $p = 0.81$). **B)** Plots show the maximum running speed during the random searching behavior. Each dot indicates the maximum running speed of each random-well-searching trial. Kruskal-Wallis test showed no significance across the session types irrespective of trials started from the non-occluded zone (left, $p = 0.31$) or the occluded zone (right, $p = 0.38$). **C)** Examples of behavior paths between the same start and goal wells across different session types (left, non-occluded; right, occluded). Start wells are indicated by filled circles in cyan (non-occluded) or magenta (occluded), and the goal (home well) locations are filled circles in red. **D)** Plot shows the variances of movement direction during goal-targeting journeys across session types. The journey time of each trial was normalized. Significantly higher variance was observed during laser application in the straight-path occluded trials ($p < 0.05$ Friedman's test), but not in the non-occluded trials ($p = 0.06$). **E)** Plots show the z-scored path length of individual goal-targeting journeys. Significant increase was observed during laser application for the trials started from the occluded zone ($p < 0.05$; Kruskal-Wallis Test) but not in those from the non-occluded zone (left, $p = 0.27$). **F)** The same plot as in D but with the z-scored time duration of goal-targeting journeys, showing significant increase during laser application in the straight-path occluded condition (non-occluded: $p = 0.13$; occluded: $p < 0.05$ in Kruskal-Wallis test).

When the animals started from the non-occluded zone, I did not find any difference either in the z-scored path length ($p = 0.27$ in Kruskal-Wallis test) or in the z-scored time duration across the session types ($p = 0.13$, Figure 3. 6E, left, and 3. 6F, left). However, both the z-scored path length and time duration changed significantly in the trials started from the occluded zone (Figure 3. 6E, right and 3. 6F, right, $p < 0.05$ in Kruskal-Wallis test). Wilcoxon rank-sum posthoc tests confirmed that the z-scored path length and time duration of goal-targeting journeys were significantly increased during

laser application compared to the control and recovery sessions ($p < 0.05$), whereas no significant difference was observed between the control and recovery session (path length, $p = 0.95$; time duration, $p = 0.99$ in Wilcoxon rank-sum test). These results together suggest that silencing of the RE impaired the animal's ability to take a smooth and short path towards the destination.

3. 3. Discussion

Although the anatomical features of the Nucleus Reuniens (RE) were characterized almost 50 years ago (Herkenham, 1978), neuroscientists' interest in the RE has grown recently because of its plausible contribution to prefrontal-hippocampal interactions supporting our higher cognitive abilities, including goal-directed navigation. However, previous studies could not find a prominent impact of RE inactivation on the animal's navigation ability (Dolleman-van der Weel et al., 2009; Ghiafeh et al.,2009; Loureiro et al.,2012). I speculated here that the lack of behavioral deficits in these previous studies is because the navigation tasks used in previous studies were inappropriate for understanding the role of the RE. I then hypothesized that the key role of the RE in navigation may reside in the ability for route planning, avoiding a known obstacle in the environment.

The experiments in this chapter confirmed my hypothesis, demonstrating that RE inactivation caused impairment in the animal's ability to take a smooth wall-avoiding route to a given destination. I found that the

animals with RE silencing often took a goal-targeting route with a longer length and duration. However, I also found that these animals with RE silencing could still accurately choose the correct goal well, suggesting that the impairment was not simply due to the deficit in goal recognition.

In my analysis, the maze was divided into two areas by an introduced wall – the straight-path occluded zone and the non-occluded zone. I found an apparent difference in the animal's navigation performance depending on whether a goal-targeting path is hindered by the wall or not. When a straight goal-targeting path was available, the animal's behavioral performance did not differ even immediately after the introduction of the wall in the maze, suggesting that the animals took the same navigation strategy irrespective of the wall insertion. However, when the inserted wall hindered the animal's straight goal-targeting path, the task performance was significantly dropped for the first few days after the wall introduction (Figure 3. 4). However, the animals learned to take a wall-avoiding route in about a week (Figure 3. 5).

Are there any differences in the animal's navigation strategy depending on whether a straight path is available or not? It is known that several animal species, including rodents, can accurately estimate a "homing' vector from their own position to the origin of navigation by accumulating instantaneous movement direction and distance during the journey – a strategy called "path integration" (Muller and Wehner, 1988). This strategy is well described in desert ants, where they can go straight back to a nest location after a long journey by relying on a homing vector.

However, this path-integration strategy does not work when a straight path to a goal is blocked by an obstacle. A homing vector provided by the path integration strategy provides an animal with an accurate estimate of goal direction and distance, but if this homing path is blocked, an animal has to come up with a detour path to avoid the obstacle. On the first few days of the wall introduction, the rats could not find the home location when a straight path to the home was blocked by the wall (Figure 3. 4). However, I noticed that, once the animals reached the edges of the wall, they could run directly toward the home location. A similar pattern of behaviors was described in desert ants (*Cataglyphis fortis*) when a goal-directed path was blocked by an obstacle (Collett et al.,2001). While ants struggle to find a way out of the obstacle, once getting out of it, they can take a straight path to the nest location.

However, the major difference from ants is that rats can learn to take a smooth wall-avoiding route even in darkness after sufficient training. This is likely the situation where the RE is necessary, and the rats start taking a navigation strategy relying on the brain's cognitive map. My finding of the animal's deficit in taking a wall-avoiding route during RE inactivation (Figure 3. 6) points to the RE's role in exploiting a cognitive map for navigational planning. Given its anatomical features, the RE likely supports this ability by transferring information from the PFC to the hippocampus. If so, what type of information is provided by RE neurons in the hippocampus?

A previous study showed that the RE is a key structure mediating the information about the animal's future movement direction from mPFC to the hippocampal CA1 (Ito et al., 2015). It is thus possible that the information

about movement directions in the hippocampus may help with route planning in a maze with an obstacle. To explore this idea further, I next tested the impact of the inactivation of hippocampal neurons on the animal's route-planning ability.

Chapter 4

Silencing of Hippocampal Neurons Impairs the Animal's Ability for Route Planning, but not Goal Recognition, in a Familiar Maze

4. 1. Introduction

Since the discovery of place cells in the rat hippocampal CA1 (O'Keefe & Dostrovsky, 1971; O'Keefe, 1976), the hippocampus has been regarded as a crucial structure for spatial navigation ability. However, this does not mean that the hippocampus is necessary for all aspects of navigation behaviors. For example, a navigation strategy relying on path integration – a way to obtain a homing vector by integrating instantaneous motions during navigation – has been well-studied in desert ants that do not have the hippocampus, and it has been shown that rats with bilateral hippocampal lesions can still take this path-integration strategy to perform successful goal-directed navigation (Alyan & McNaughton, 1999).

However, each navigation strategy has a drawback. For example, a navigation strategy relying on the sunlight direction cannot be used under a cloudy weather condition, and a path integration strategy does not work if a path along a homing vector is blocked by an obstacle. In *Chapter 3*, I discovered that RE inactivation impaired the animal's ability to take a wall-

avoiding path to a home location, but the same manipulation did not cause any apparent navigation deficit in the open maze without obstacles, suggesting that RE plays a key role in navigation particularly when a path integration strategy does not work.

It is known that the hippocampal CA1 receives a strong input from the RE (Dolleman-van der well & Witter, 2000; Bokor et al., 2002), and the previous study showed that the RE mediates information transfer from the prefrontal cortex to the hippocampal CA1, enabling place cells to represent the animal's next movement direction (Ito et al., 2015). This information transferred from the RE to the hippocampus may support the animal's ability for route planning.

However, the exact contribution of the hippocampus to navigation has not yet been clear. Given the precise spatial tuning of place cells, the hippocampus may be essential for an animal to recognize its own position accurately. Another possibility is that information in the hippocampus about a spatial layout of the environment may help an animal to estimate the positions of environmental landmarks, such as obstacles or boundaries.

To determine the role of the hippocampus in navigation, I took advantage of our newly-designed navigation task (see Methods and *Chapter 3*) because this task allows us to assess the animal's ability for route planning by avoiding a known obstacle in the maze. Here, I inactivated neurons in the bilateral hippocampus and examined its impact on the animal's performance in this task.

4. 2. Result

4. 2. 1. The DREADDs system allowed for reversible inactivation of neurons in the bilateral hippocampi

I took a chemogenetic approach to inhibit the neural activity in the hippocampus. I thought that the optogenetic method is not ideal for this purpose because of limited light application to a large volume of the hippocampus. In the strategy of Designer Receptors Exclusively Activated by Designer Drugs (DREADDs), engineered G-protein coupled receptors are activated by a high-affinity selective agonist deschloroclozapine (DCZ) (Nagai et al., 2020). For example, this agonist can suppress the spiking of neurons expressing human muscarinic acetylcholine receptor DREADD subtype 4 (hM4Di) (Armbruster et al., 2007). I injected an AAV encoding hM4Di and mCherry under the hSyn promoter in the bilateral hippocampi along the entire dorsoventral axis (Figure 4. 1A). The virus expression is shown in green in the 3D reconstructed image from the serial block-face microscope sections (Figure 4. 1B).

Three to four weeks after the virus injection, the activity of neurons in the hippocampus was recorded to confirm the impact of the agonist DCZ injection. The animal received the agonist DCZ subcutaneously, and the time series of individual neurons' firing rates were normalized to the mean rates during the first 5 minutes following the agonist injection (Figure 4. 1C). A subset of cells exhibited a significant decrease in firing rates to less than 50% of the baseline at approximately 30 minutes after the agonist injection.

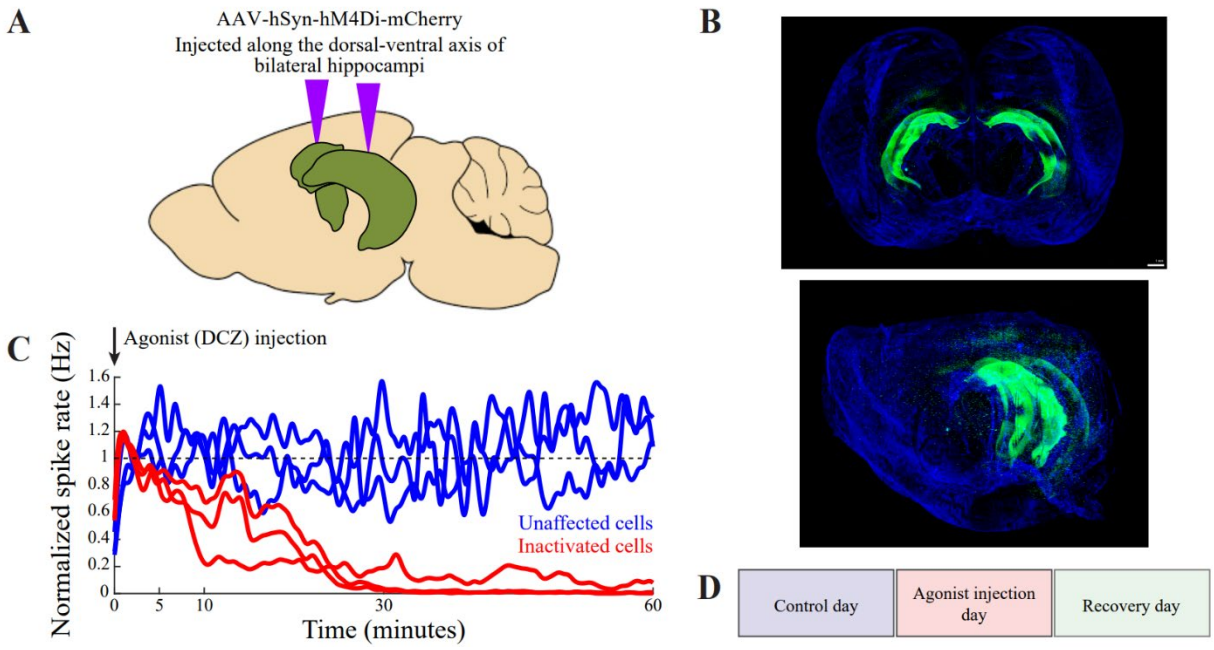

Figure 4. 1. The activity of neurons in the bilateral hippocampi were suppressed by the DREADDs method.

A) AAV encoding inhibitory DREADDs hM4Di and red fluorescent protein mCherry under the hSyn promoter were injected into the bilateral hippocampi. **B)** 3D reconstructed images of brain sections with mCherry expression in green and DAPI staining in blue. Top, coronal view; bottom, sagittal view. **C)** Plot shows spike rates of 6 representative hippocampus neurons after agonist (DCZ) injection. By 30 minutes after the injection, the firing rates of a subset of neurons decreased to a level less than 50% of baseline firing (red). **D)** Scheme of the experimental design. Each set of experiments was conducted over three consecutive days, each of which was for control, agonist, and recovery session.

A set of behavioral experiments was designed across three consecutive days, considering the fact that the complete washout of the agonist takes 24 hours after the injection. I compared the animal's task performance day by day. On the first day of experiments, the animals performed the task 1 hour after the subcutaneous injection of the vehicle (water for injection). On the second day, the same animals received the injection of the agonist 1 hour

before the task. On the third day, the animals performed the task without any injection.

The task rule and conditions were the same as in the experiments in the previous *Chapter 3*. Behavioral data were collected from two different home locations. The animal's position was monitored by using the two LEDs located on the animal's head.

4. 2. 2. Animals with hippocampal inactivation took a longer wiggled behavior path

To assess the impact of hippocampal inactivation, I applied the same analyses as in the previous *Chapter 3* for the RE inactivation experiments. I first examined the percentage of correct home-targeted trials for each session and did not find any significant impact of the hippocampal inactivation (Figure 4. 2A; non-occluded $p = 0.12$; occluded $p = 0.24$ in Kruskal-Wallis test). I did not find any difference between the non-occluded and the occluded conditions either ($p = 0.10$ in Kruskal-Wallis test). This result is surprising because, unlike previous studies suggesting the key role of the hippocampus in navigation, the hippocampus can be dispensable for the accurate recognition of goal location.

I then analyzed the maximum running speed of the animal during random foraging trials (Figure 4. 2B). A statistical test did not reveal any significant change during the hippocampal inactivation (Figure 4. 2B; non-occluded, $p = 0.10$; occluded, $p = 0.95$; Kruskal-Wallis test) or between the non-occluded and the occluded conditions ($p = 0.37$ in Kruskal-Wallis test),

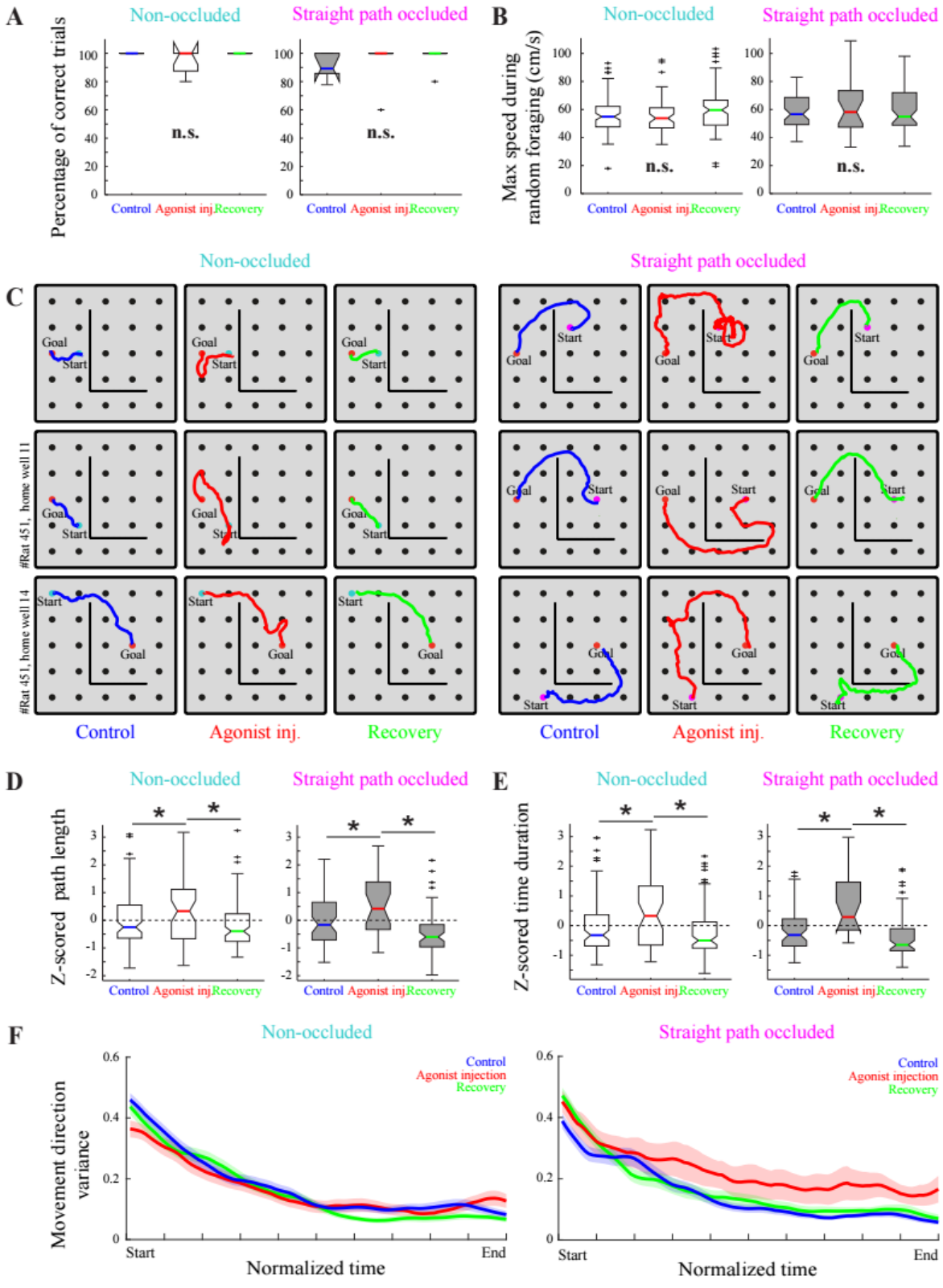

Figure 4. 2. Bilateral hippocampal inactivation caused the rat to take a non-smooth longer path to the goal regardless of the relation between the start and the goal location.

A) Plots show the task performance - the percentage of home-targeted trials without erroneous

licks of other wells. Each dot indicates the percentage of correct trials in each session. No significant difference between sessions was observed (non-occluded, $p = 0.12$; occluded, $p = 0.24$; Kruskal-Wallis test). **B)** Plots show the maximum running speed during the random foraging trials. Each dot indicates the maximum running speed in each random trial. No significant difference was observed (non-occluded $p = 0.10$, occluded $p = 0.95$; Kruskal-Wallis test). **C)** Examples of behavior paths between the same start-goal pairs across individual sessions. The start wells are indicated in cyan (left, non-occluded) or magenta (right, occluded) and the home wells (no.11 and 14) are in red. **D)** Plots show the z-scored path length of home-targeted journeys. Each dot corresponds to each trial data. Significant increase in the path length was observed in the days with agonist injection ($p < 0.05$; Kruskal-Wallis test with postdoc Wilcoxon ranksum test). **E)** Plots are for the z-scored time duration of goal-targeting paths. Significant increase in time duration was observed in both occluded and non-occluded conditions during the hippocampus inactivation ($p < 0.05$; Kruskal-Wallis test with a posthoc Wilcoxon ranksum test). **F)** Plots show time series of movement-direction variance during goal-targeting journeys. The journey time of each trial was normalized. The variances were significantly larger on the agonist injection days when the animals started from the occluded zone ($p < 0.05$; Friedman's test) but not when they started from the non-occluded zone ($p = 0.51$).

suggesting that the manipulation did not affect the animal's movement ability in general.

However, I found an apparent difference in the animal's home-targeting path during the hippocampal inactivation. Although the animals took a smooth wall-avoiding home-targeting path on the control and the recovery days (blue and green), they took a more wiggled inefficient path on the agonist injection day when hippocampal neurons were inactivated.

To quantify the differences in home-directed paths, I calculated the z-scored path length, the z-scored time duration, and the variances of movement direction during the goal-targeting journeys. I found a significant increase in both path length and time duration of goal-targeting journeys on the agonist injection days in both the occluded and the non-occluded conditions. (Figure 4. 2E and 2F, $p < 0.05$ in Kruskal-Wallis test and posthoc Wilcoxon ranksum test). Furthermore, the hippocampal inactivation increased the variances of the animal's movement direction when a straight-goal-targeting path was blocked by the wall ($p < 0.05$; Kruskal-Wallis test), but not when the journeys started from the non-occluded zone ($p = 0.51$). Notably, unlike the cases of RE inactivation, the differences in the animal's behavior paths were observed even when the journeys started from the non-occluded zone. Furthermore, the increase in movement variances was not limited to the initial phase of the journeys, but observed across the entire duration of navigation.

4. 3. Discussion

In this chapter, I investigated the role of the hippocampus in goal-directed navigation. To my surprise, the animal's ability to find the right goal location was not impaired even after the inactivation of neurons in the entire bilateral hippocampi. The animal did not lick wrong wells, suggesting that the animal was able to recognize the correct goal location even without the hippocampus. The animal's ability for goal recognition can thus be supported

by other brain regions, such as the entorhinal cortex and the orbitofrontal cortex (Basu et al., 2021; Hafting et al., 2005).

Despite the fact that the animal can accurately recognize the goal location, the hippocampus inactivation caused the animals to take a longer wiggled path (Figure 4. 2), suggesting an impairment in the ability for route planning as observed in animals with RE inactivation (*Chapter 3*). However, unlike the cases in RE inactivation, the hippocampus inactivation induced this deficit, not only when the journeys started from the occluded zone, but also when they started from the non-occluded zone. This observation suggests that the behavioral deficit caused by hippocampal inactivation is not limited to planning the wall-avoiding path. From the results of the movement-direction variances, I found that the hippocampal inactivation increased the variances along the entire journey when it started from the occluded zone, which is again different from the cases in the RE inactivation where the higher variances were observed only at the initial phase of the journey. The movement-direction variance calculation in non-occluded conditions shows that the animals with hippocampal inactivation were able to head toward the goal direction smoothly. However, the animals still took a longer path in length and time, suggesting some degree of impairment.

These results suggest that these animals with hippocampal inactivation still have the ability to estimate a rough goal direction (that's why behavior paths were smooth) but likely have a problem in accurate targeting to a particular location. This is not simply due to the inaccurate estimation of the goal location because they did not lick the wrong wells. It is rather likely

because of the problem in updating the precise spatial relationships between the self's position and the target location during navigation.

The hippocampus has been regarded as a crucial structure for navigation, and previous studies investigated the role of the hippocampus not only in animals, but also in humans. Several experiments have been performed to test the navigation ability of human patients with damage in the hippocampus. However, the exact contribution of the hippocampus to spatial navigation is still controversial because of the inconsistency between the navigation performance and the hippocampal pathology of patients.

It was reported that patients with hippocampal lesions were able to describe an appropriate path to a given goal location at the same level as healthy subjects (Teng & Squire, 1999; Rosenbaum et al., 2000), but other studies reported a major deficit in spatial navigation ability caused by the damage in the hippocampus (Vargha-Khadem et al., 1997). While these results may look contradictory, the tests in the former studies were performed based on the familiar environment where they grew up, but the latter was not. For example, the patient H.M., who received surgical resection of the bilateral medial temporal lobes, could describe the spatial layout of a familiar environment where he lived for more than ten years (Corkin, 2002) but exhibited impairment in performing other spatial memory tasks (Milner, 1965; Corkin, 1965). These results together indicate that the hippocampus may be dispensable for navigation in a familiar environment.

Does the hippocampus play any role in spatial navigation in a familiar environment? The patient K.C. with severely-reduced hippocampus volume,

could retrieve fewer landmarks in the environment than control subjects (Rosenbaum et al., 2000), even for the ones experienced in his neighborhood. Another patient E.P., who had extensive bilateral damage to the medial temporal lobe including the hippocampus, knew the landmark locations verbally but could not head toward these landmark positions (Teng & Squire, 1999). Because the tests in these studies were conducted based on a familiar environment for the patients, the hippocampus may particularly be important for memorizing environmental landmarks. Furthermore, a positron emission tomography (PET) study showed that the human hippocampus was active more in successful navigation than unsuccessful navigation in a familiar environment in a virtual reality setting (Maguire et al., 1998), serving as another piece of evidence that the hippocampus is involved in navigation even in a familiar environment.

Information about environmental landmarks is crucial for map-based navigation. For example, it is known that information about boundaries is considered to be important to anchor the brain's internal map to the environment for accurate position estimation (Hardcastle et al., 2015). However, even without landmark information, we can often take alternative strategies for successful navigation. For example, we can memorize a particular route to the destination, and correspondingly, it has been shown that the human perirhinal cortex showed higher activity when taking the same familiar route rather than new paths (Hartley et al., 2003), suggesting non-hippocampal brain region may support a navigation strategy based on route memory. To avoid these potential confounds in different navigation strategies, I performed all the navigation experiments in darkness and changed the

home-well location in the maze, so that the animal must come up with an appropriate goal-directed route by relying on the brain's internal map. The key landmarks in my experiments were the boundaries at the square box peripherals as well as the inserted wall. When the hippocampus was inactivated, the animals exhibited difficulty in taking a smooth short wall-avoiding path, which may have resulted from inaccurate estimation of these landmark locations.

Consistent with our observations, it was described that a patient with reduced bilateral hippocampal volume by 30% (Olsen et al., 2013) showed significant impairment in describing the locations of landmarks and in finding the shortest detour between two landmarks (Rosenbaum et al., 2015). Another study using a virtual-reality setup reported that the activation of the hippocampus is highly correlated with a successful discovery of efficient routes in distance and time (Hartley et al., 2003).

Altogether, previous studies in humans as well as my results in this chapter suggest that the hippocampus is necessary for landmark memories, which may support the ability for route planning to avoid known obstacles in the environment. In the previous chapter, I confirmed that silencing RE neurons caused impairment in taking a smooth obstacle-avoiding route. I here observed a similar behavioral deficit by hippocampus inactivation, suggesting that the RE-hippocampus projection plays a key role in the planning of navigational routes adapted to a spatial layout of the environment.

My next question is about the neural mechanisms by which the hippocampus supports the planning of future navigational routes. As a hint

for this mechanism, previous studies reported that the activity of hippocampal neurons is sometimes correlated with the animal's future or past trajectories in navigation (Foster & Wilson, 2006; Diba & Buzsaki, 2007). These trajectory representations among place-cell ensembles are primarily observed when the animals are stationary before starting navigation (Pfeiffer and Foster, 2013). If such future trajectory coding in the hippocampus is necessary for accurate route planning, impairment of this process by the RE inactivation may cause a navigational deficit. To test this possibility, I recorded the activity of hippocampal neurons while the animal performed the same spatial navigation task, and analyzed trajectory representations in the hippocampus before starting navigation.

Chapter 5

The Nucleus Reuniens Drives Goal-directed Trajectory Sequences in the Hippocampus

5. 1. Introduction

In the previous chapter, I confirmed that the inactivation of the nucleus reuniens (RE) or the hippocampus resulted in a similar impairment in navigation ability. These animals were still able to discriminate the goal well from other wells once it reached there. However, they showed difficulty in locating the goal location from different start positions by taking an efficient route. Consistent with this observation, the projections of RE neurons to the hippocampal CA1 have been shown to be necessary for CA1 neurons to represent the animal's future movement direction (Ito et al., 2015), implying that the RE-CA1 circuits may play a key role in a route planning process.

Neurons in the hippocampus increase their firing when an animal visits a particular location in space, often called place cells. Several studies further showed that the place cells do not only indicate the animal's own position, but sometimes represent the animal's future navigational state (Skaggs & McNaughton, 1996; Foster & Wilson, 2006; Diba & Buzsaki, 2007). For example, CA1 place cells change their firing rates before the upcoming T-

junction of the maze, representing the animal's future turning direction (Wood et al., 2000; Ito et al., 2015). Furthermore, when the animal is in an immobile state, place cells do not necessarily represent the animal's own position anymore, but instead indicate a position away from the animal. Pfeiffer and Foster (2013) have shown that the activity of place cells before the onset of a goal-directed journey depicts the animal's upcoming path toward the next destination.

Because neurons in the RE project to area CA1 of the hippocampus and the subiculum (Herkenham, 1978; McKenna & Vertes, 2004), I reasoned that the impairment of navigation ability by RE silencing may be due to its impact on goal-directed trajectory sequences generated in the hippocampus. To test this hypothesis, I recorded the activity of neurons in the hippocampal CA1 and examined their representing positions before starting a goal-directed journey. By implementing simultaneous recordings and optogenetic manipulations, I investigated the impact of RE silencing on the generation of goal-directed sequences in the hippocampal CA1 and its associated impairment in the animal's route-planning ability, as explored in *Chapter 3*.

5. 2. Results

5. 2. 1. Decoding of the animal's position from the activity of hippocampal CA1 neurons

To record the neural ensemble activity in hippocampal CA1, a tetrode microdrive with 28 individually movable tetrodes was implanted in the

bilateral hippocampus. Rat 335 and 509 received the injection of AAV encoding the inhibitory opsin SwiChR++ together with an optic fiber in the RE (Figure 5. 1A). After the surgery, all the tetrodes were slowly moved down until they reached the pyramidal layer of the hippocampus, which could be assessed by the characteristics of sharp-wave ripple waveforms as well as the existence of burst spiking neurons (Figure 5. 1B).

More than 200 cells were simultaneously recorded during the task. The structure of daily sessions was the same as in the behavioral experiments in *Chapter 3*, and the duration of individual recording sessions was 15~20 minutes. Due to the animal's reduced motivation and neuronal instability, I did not perform the analyses of the recovery sessions. I recorded a consistent number of place cells (Figure 5. 1C) across session types (Figure 5. 1D, $p = 0.88$ in Wilcoxon rank sum test) and confirmed that the RE inactivation did not change spatial tunings of individual neurons ($p = 0.08$ in Kruskal-Wallis test), suggesting that the same hippocampal spatial map is maintained irrespective of RE activity.

A Bayesian decoder was constructed to examine trajectory sequences represented by the activity of ensemble hippocampal neurons. The maze arena was divided into 2.5 cm x 2.5 cm bins. Firing rates of individual neurons at each position bin were averaged when the animal's running speed exceeded 5 cm/s. These mean firing rates of all neurons at individual position bins allow us to take a Bayesian approach to estimate the most-likely position given a set of firing rates of the same neurons. I confirmed that this approach was able to estimate the animal's position accurately while it explored the maze with a running speed of over 5 cm/s (Figure 5. 3A).

The same position decoder was applied to the neural activity while the animal licked individual wells and when the animal's running speed was less than 5 cm/s. Because of the time compression in the sequential firing of hippocampal neurons (Lee & Wilson, 2002), I estimated a position

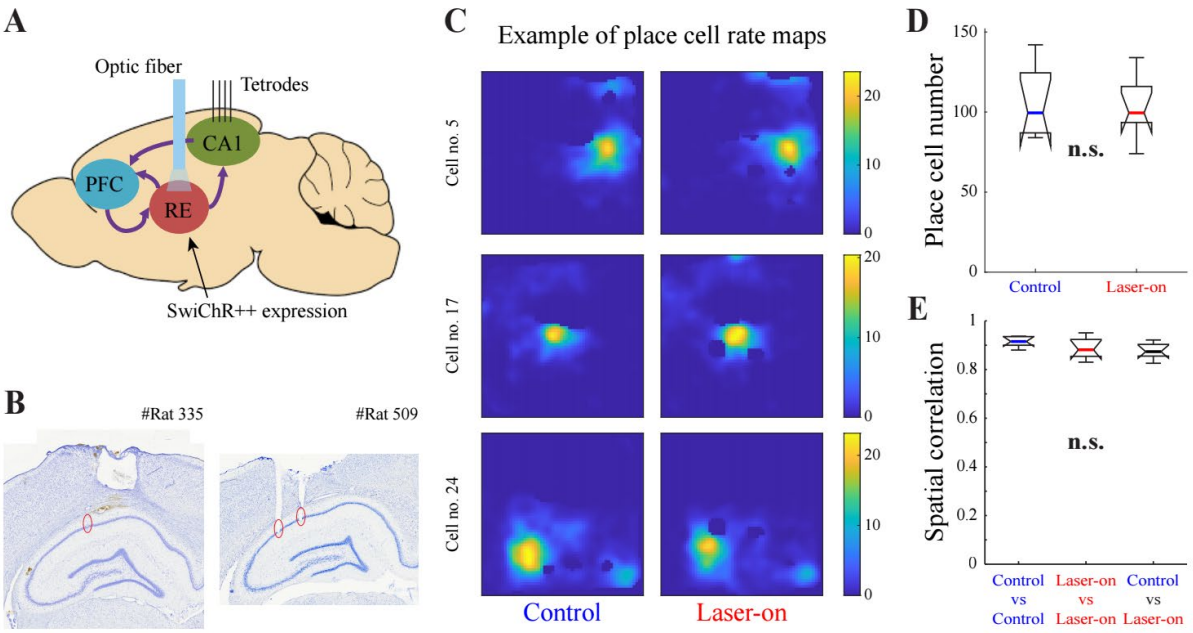

Figure 5. 1. Hippocampal CA1 neuronal ensemble activity recorded with multi-tetrodes drive

A) The animals used in *Chapter 3* for RE silencing had multi-tetrodes drive implantation in the hippocampal CA1. **B)** Tetrodes positions in the hippocampal CA1. The end of tetrode tracks marked in red circles. Left, rat 335 and right, rat 509. **C)** Example of position spike rate maps of place cells from one recording data set from rat 509. Left column, position spike rate maps in the control session, and right column, rate maps of the same cell in the laser-on session. The color range of heatmaps is the same across different sessions within each cell. **D)** Place cell number of each data set. Place cell was classified if the spatial correlation was exceeded 0.6. No significant difference was observed between control and laser-on session ($p = 0.88$ in Wilcoxon rank sum test). **E)** Spatial correlation value averaged among all recorded cells in each session (see Methods). No significant difference observed between session types and the comparison between control and laser-on session ($p = 0.08$ in Kruskal-Wallis test).

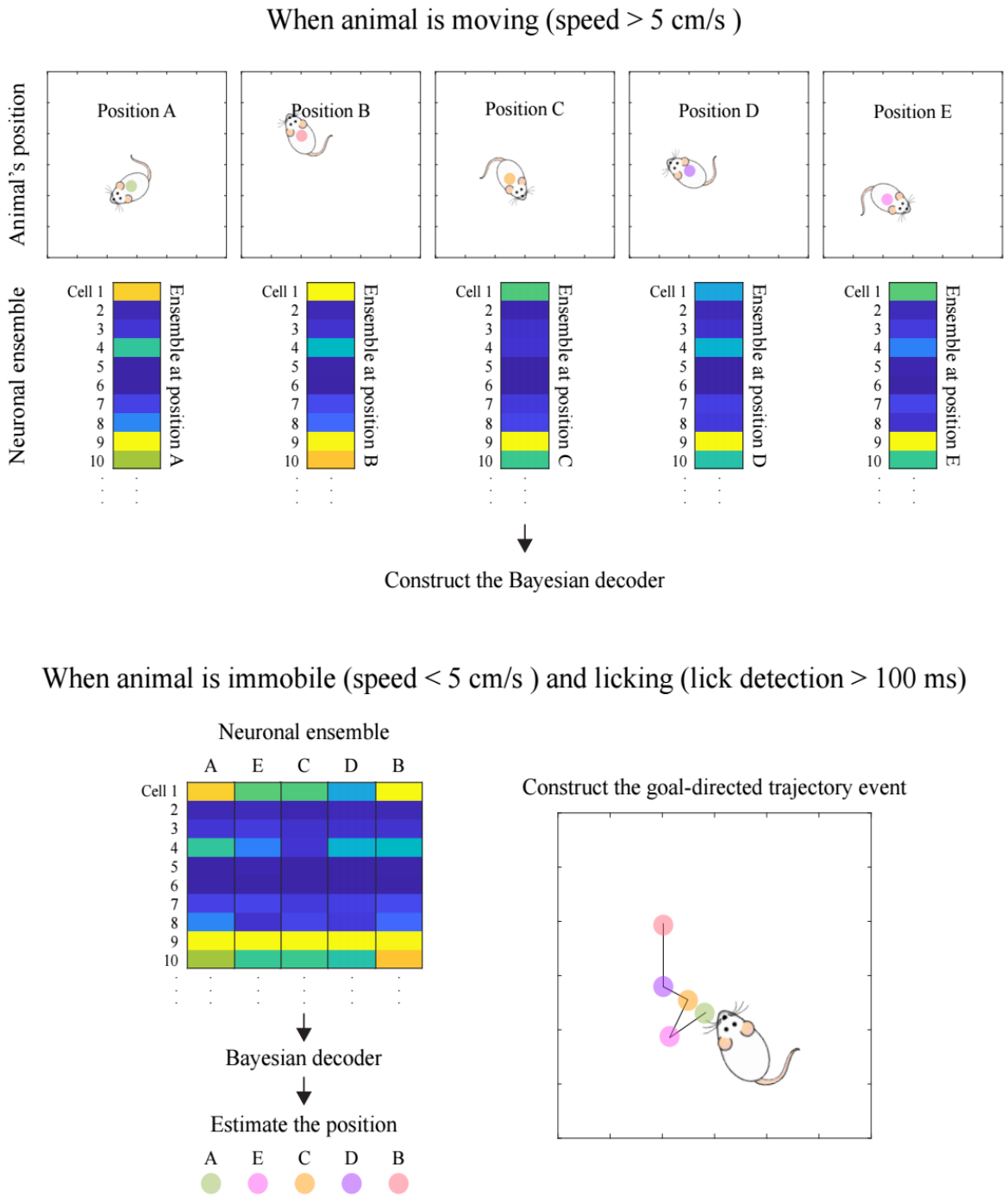

Figure 5. 2. Scheme of replayed trajectory events detection methods using the Bayesian decoder

The position spike rate matrix was constructed with the neuronal ensemble data when the animals moved above 5cm/s speed. Each position bin is assigned to the neuronal ensemble. The Bayesian decoder was constructed with this position spike rate matrix. When the animals were immobile and licking the wells, a neuronal ensemble was put into the constructed

Bayesian decoder to estimate the represented position. If the decoded position sequences are away from the animals' current position, those sequences were detected as replayed trajectory events.

represented by the activity of hippocampal neuron ensembles in a short time bin of 20 ms, which was time-shifted at every 5 ms. The decoded positions constituting a position sequence in the maze that spanned at least 25 cm away from the animal's position are considered trajectory events (Figure 5. 2; see Methods for details).

To assess the impact of RE silencing, I first asked whether RE silencing has an impact on the place cell's coding of the animal's position during active maze exploration. I constructed a Bayesian position decoder based on the recording data in each daily session, and compared its mean decoding errors between the control and the laser-on sessions. I did not find any significant difference in the performance ($p = 0.38$, Wilcoxon rank sum test), suggesting that the RE silencing did not affect the position-coding of place cells in the hippocampus.

5. 2. 2. RE inactivation diminished goal-directed trajectory events

To assess the impact of RE on trajectory events, the Bayesian position decoder constructed from the neural activity during the maze exploration was applied to the neural activity while the animal licked wells. To analyze the goal-directed trajectory events in the home-targeting phase of the task, I split the events based on the starting positions, either when the animal started from

the non-occluded or the occluded zone (Figure 5. 4A). I analyzed the rates of trajectory events and did not find any significant difference between the non-occluded and the occluded zones nor between the control and the laser-on sessions (control, $p = 0.08$; laser-on, $p = 0.70$; non-occluded, $p = 0.92$; straight path occluded, $p = 0.26$ in Wilcoxon rank sum test).

To assess the behavioral relevance of the detected trajectory events, I normalized all the events so that the start and the goal locations are aligned

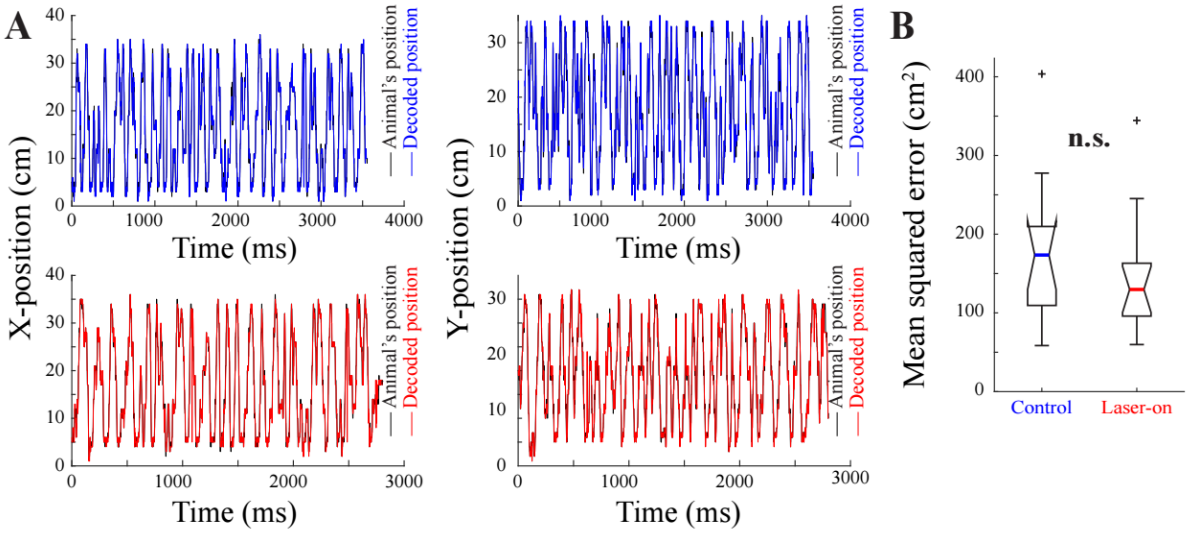

Figure 5. 3. The Bayesian decoder successfully decodes animal's position with and without intact RE

A) The Bayesian decoder estimated the animal's position when the animal actively moved above the speed criteria (> 5cm/s). Top, blue is the decoded position, and black is the animal's actual position data in the control session (left, x positions; right, y position). Bottom, red is decoded position and the others are the same as the top panel from the laser-on session. The x-axis is the position bin and the y-axis is the total time the animals were actively moving in milliseconds. **B)** Mean squared error (cm^2) between decoded and actual position. There was no significant difference between the control and laser-on sessions ($p = 0.38$ in the Wilcoxon rank sum test).

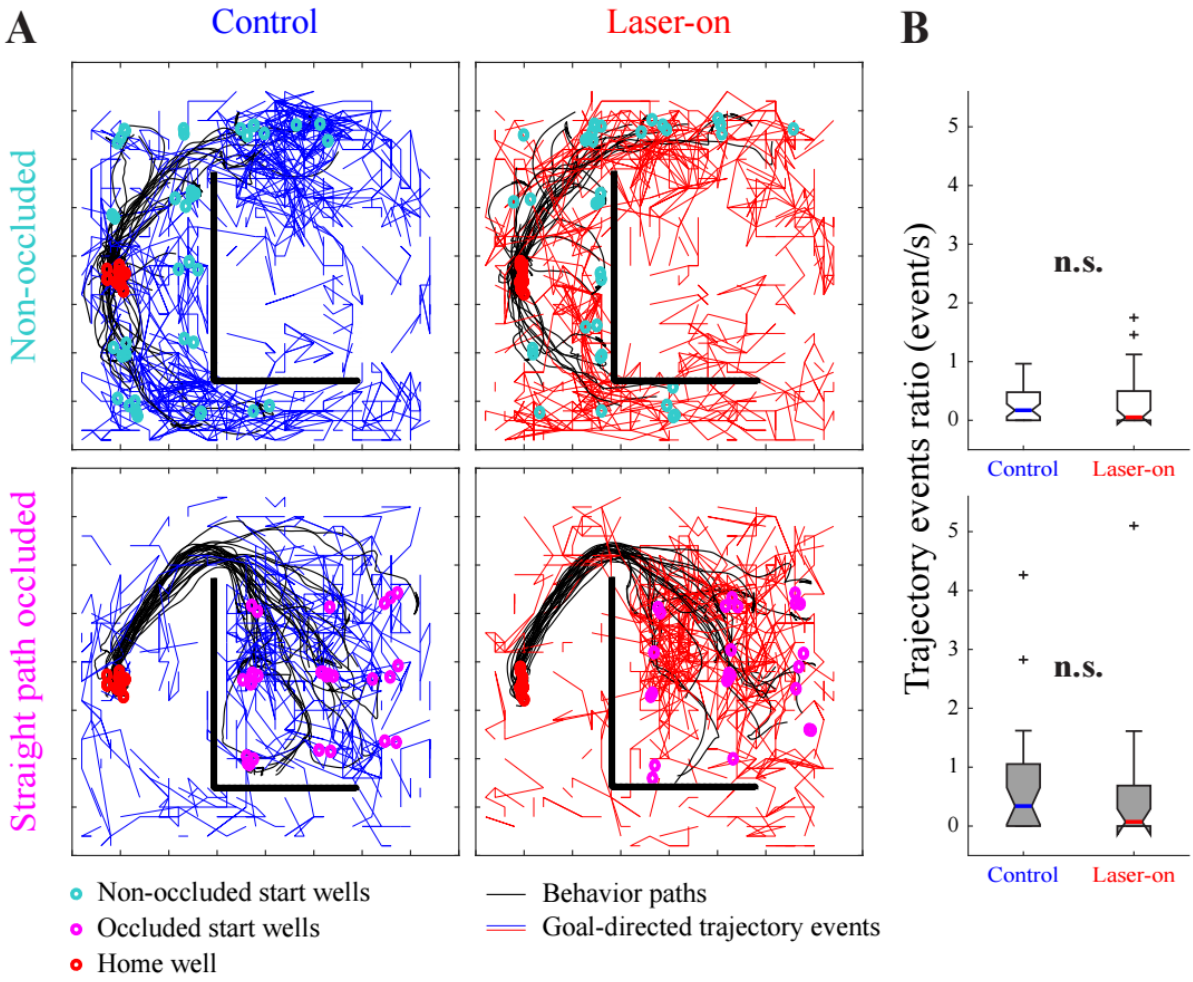

Figure 5. 4. Goal-directed trajectory events were detected during the random reward licking before the start of the home trial

A) The detected goal-directed trajectory events are represented by a colored line in the maze space (left, control session, in blue line; right, laser-on session, in red line). The position of the L-shaped wall is indicated by a thick black line. The thin black lines are the behavior paths after detection of the trajectory events. The start positions of the behavior paths are marked by cyan (top, non-occluded) or magenta (bottom, straight path occluded) colored circles. The goal positions of the behavior paths (home well positions) are marked with red circles. **B)** The ratio of the goal-directed trajectory events was calculated per session as the number of events divided by the total stationary time (event/s). No significant difference was observed in the ratio of replayed events between session types (top, non-occluded, $p = 0.92$; bottom, straight path occluded, $p = 0.26$ in Wilcoxon rank sum test).

for the subsequent goal-targeting journeys (Figure 5. 5A). In our task design, the animals are required to switch their navigation strategy between random-well-searching and home-targeting phases. This switch is likely to be elicited by a sound cue and water delivery at the time when the animal licked a correct random well for at least 300 ms, because the animal should subsequently stop random-well searching and start planning a subsequent goal-targeting journey.

I thus divided trajectory events into two categories. One is the foraging events generated during the animal's well lickings in a random-searching phase of the task, from the time of the animal's leave from the home well until the threshold (300 ms) of the well licking at a correct random well. Another category is the homing events that happen after the threshold time of the correct-random well licking until the animal leaves this well. In support of this prediction, I found a prominent difference between the foraging and the homing trajectory events. The foraging events are mostly localized near the animal's position and I did not observe a particular bias toward the home location. By contrast, the homing events exhibit significantly biased representations at the home well (Figure 5. 5A). To quantify the differences, I calculated the density of represented positions by the trajectory events along the start to the home locations. When comparing the ratio of event density between the animal's position and the home-well location, I found the ratio is significantly larger in the homing events compared to that of the foraging ones (Figure 5. 6). This difference is observed irrespective of whether the journeys started from the non-occluded zone (Figure 5. 5C left line graph, $p < 0.05$ in binomial test) or the occluded zone (Figure 5. 5C left, $p < 0.05$ in

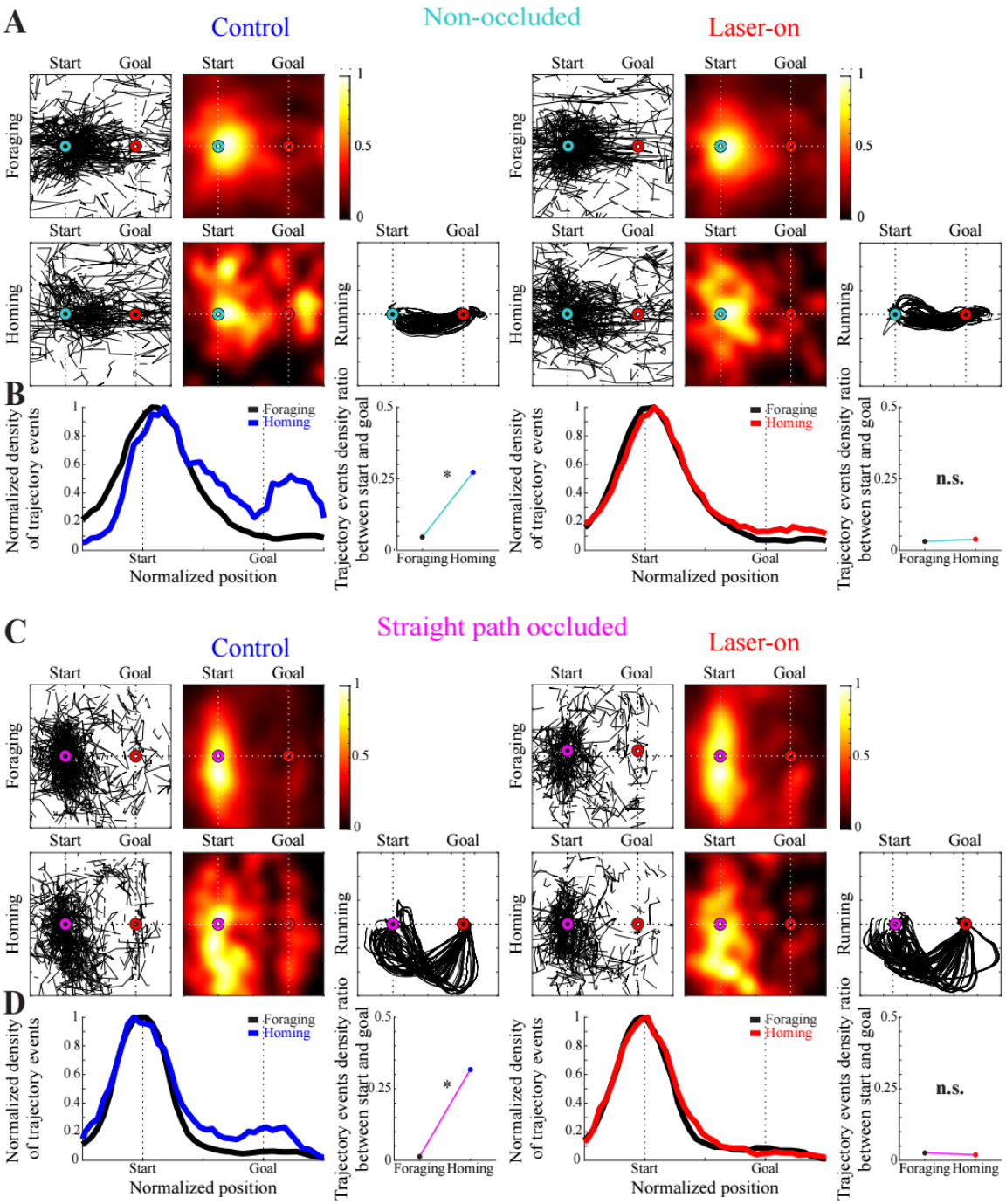

Figure 5. 5. Population activity of goal-directed trajectory events biased towards the future goal location when planning a subsequent goal-targeting journey but diminished with RE silencing

A) Normalized and aligned detected goal-directed trajectory events (black lines) according to the relation of the current animals' position and the future goal location from non-occluded start wells. The start wells are marked in cyan circles, and the future goal location (home wells) are

marked in red circles. The top row, foraging events with randomly selected trajectory events example with the same number as in homing events for the visualization. Line plots, each black solid line is goal-directed trajectory events. Right heatmap plots, the density of the trajectory events is depicted in a color range of 0~1, which is normalized by the maximum density of each plot. Right bottom corner, the behavior paths of following goal-targeting journey also normalized and aligned. **B)** The density of goal-directed trajectory events was calculated in a range of 0.5 along the horizontal axis in the normalized space. The density was normalized with the peak of each graph. The normalized density of foraging events represented in a black line and of homing events in a color line (left, control session in blue; right, laser-on session in red). The dotted line indicates the start and the goal in the normalized position. The line graph represents the trajectory event density ratio between the start and the goal, calculated as the sum of the normalized density of trajectory events within the 0.1 size bin in the normalized space at the start. The ratio between foraging and homing events was significantly different in the control session but not in the laser-on session (left, control, $p < 0.05$; right, laser-on, $p = 0.71$ in binomial test). **C and D)** The same plot as A and B at straight path occluded start wells. The start well indicated in magenta circle. The trajectory event density ratio between start and goal was significantly different in the control session but not in the laser-on session (left, control, $p < 0.05$; right, laser-on, $p = 0.68$ in binomial test).

binomial test). The results support the idea of quantitative changes in representations at the home well (Figure 5. 5A). To quantify the differences, I calculated the density of represented positions by the trajectory events along the start to the home locations. When comparing the ratio of event density between the animal's position and the home-well location, I found the ratio is significantly larger in the homing events compared to that of the foraging ones (Figure 5. 6). This difference is observed irrespective of whether the journeys started from the non-occluded zone (Figure 5. 5C left line graph, $p < 0.05$ in binomial test) or the occluded zone (Figure 5. 5C left, $p < 0.05$ in

binomial test). The results support the idea of quantitative changes in trajectory events generated in the hippocampus, starting to represent the next navigational goal prior to the onset of the journey.

I then examined the impact of RE inactivation on trajectory events and found that a goal-directed bias in the homing events was largely diminished during RE inactivation (Figure 5. 5A and C, right). This impairment was observed irrespective of whether the journeys started from the non-occluded zone (Figure 5. 5B right line graph, $p = 0.71$ in binomial test) or the occluded zones (Figure 5. 5D right, $p = 0.68$ in binomial test). The results suggest that the RE activity is essential for hippocampal neural ensembles to generate goal-directed trajectory sequences toward the next navigational goal.

5. 3. Discussion

In previous *Chapter 3*, I found the role of the RE in supporting the animal's ability to plan an obstacle-avoiding route to the destination. Because the RE is considered an anatomical hub to transfer information from the prefrontal cortex to the hippocampal CA1, I predicted RE inactivation to have a major impact on the activity of hippocampal neurons, and this RE-dependent activity modulation may support the animal's ability for route planning. In support of this hypothesis, I confirmed that the inactivation of bilateral hippocampi results in a similar route-planning impairment as observed in the animals with RE inactivation.

My question in this chapter is to understand the exact impact of the RE on the spatial coding in the hippocampus. By using a microdrive with individually movable tetrodes, I successfully recorded from more than 200 hippocampal neurons together with the optogenetic manipulation of the activity of RE neurons simultaneously. While the animal explored the maze, I did not find any significant difference in the spatial tuning of place cells, allowing me to decode the animal's position accurately, irrespective of the activity of RE neurons. I then analyzed the trajectory events generated while the animal licked the wells.

Consistent with a previous report (Pfeiffer and Foster, 2013), I observed goal-directed trajectory sequences before the onset of the animal's home-directed journeys. I also found that these sequences avoided the inserted wall despite the fact that the animal was not able to see the walls from the starting position, suggesting that these activities may support the planning a wall-avoiding route in darkness. I further explored whether the contents of hippocampal trajectory events may change depending on the behavioral demands of the task. I divided all the events into two categories, the foraging and the homing events, based on the time at which the animals should switch a behavioral strategy from random-searching (foraging) to goal-targeting navigation (homing).

In control sessions, I found that homing events exhibit a significantly higher density near the home-well location. However, this difference largely diminished in the laser-on sessions. These results indicate that RE activity is likely essential for hippocampal neural ensembles to change the contents of trajectory events corresponding to the navigational demands in the task. I also

found that this impact on trajectory events was observed irrespective of whether the journeys started from the occluded or non-occluded zones, implying that the general role of the RE is to impose a goal-directed bias in trajectory events prior to a goal-targeting journey.

On the other hand, the behavioral analyses in *Chapter 3* suggest that a significant impairment was observed only when the animal's journeys started from the occluded zone. These inconsistencies imply that goal-directed trajectory sequences in the hippocampus become indispensable only when the animals are required to avoid known but unseen obstacles to reach a destination. If the goal can be reached by taking a straight path, other brain regions may be able to support this journey even without goal-directed sequences in the hippocampus.

Altogether, my results suggest that the RE plays a key role in supporting the animal's ability for route planning when a straight goal-targeting path is blocked by an obstacle. The inputs from RE neurons in the hippocampus are essential for hippocampal neural ensembles to generate goal-directed trajectory sequences before starting the next journey, supporting the animal's planning of obstacle-avoiding paths to a desired destination.

Chapter 6

Conclusions and Future Perspectives

Navigation is an essential ability for animals to survive in space. Each animal uses a navigation strategy that suits its lifestyle and environment. Among them, a navigation strategy relying on the brain's internal map (or cognitive map) is thought to be useful for animals living in a complex environment to find a route to their destination by avoiding obstacles. Planning a shorter route is crucial for saving time and energy, but this process has not been well investigated so far. In this dissertation, I conducted experiments and analyses to clarify necessary brain regions and neural coding mechanisms to represent upcoming navigational routes avoiding obstacles, and identified the PFC-RE-CA1 circuit as crucial for route planning in navigation.

I first examined the impact of RE silencing on the rat's ability for a spatial navigation task requiring obstacle-avoiding route planning (*Chapter 3*). The RE-silenced animals could recognize the goal locations correctly but showed significant impairment in finding a short and smooth obstacle-avoiding path. Notably, I did not observe an effect of RE silencing when a

straight path to the goal was available, suggesting a specific role for the RE in route planning. I then investigated the role of the hippocampus in navigation (*Chapter 4*). While the animals with bilateral hippocampal silencing maintained the ability to recognize the goal location, these animals exhibited an impairment in finding a short and smooth goal-directed path. However, unlike the RE-silenced animals, the route-planning impairment of hippocampal-inactivated animals was observed irrespective of whether a straight path to the goal was occluded or non-occluded. This difference between the silencing of RE and the hippocampus is likely because the hippocampus has a broader function for an animal to recognize its own position as well as landmark locations. I then examined the difference in neural population activity in the hippocampus with and without RE inactivation (*Chapter 5*). I analyzed and compared trajectory sequences represented by hippocampal neurons before starting navigation, and found a significant goal-directed bias during the homing phase compared to the foraging phase of the task. I further discovered that the goal-directed bias of trajectory sequences during the homing phase was reduced by RE inactivation, likely associated with impaired route planning in these animals.

Several discoveries in this project rely on the design of a behavioral task. The newly designed task in this project has several features to answer my question of whether and how the animal plans a navigational route avoiding known but unseen obstacles in the environment using a cognitive map. First, the insertion of walls changed the maze environment from an open field to a more complex environment, forcing animals to take obstacle-avoiding paths. The necessity of 2-3 training days for the rats to take a smooth

and short wall-avoiding route suggests the brain's additional demand for implementing this navigation strategy. Consistent with this speculation, I found a specific contribution of the RE here. Second, the behavioral task contains two distinct phases – random searching and goal targeting. The animals could recognize a transition between the two phases by a beep sound and reward delivery. This clear distinction between the two task phases allowed us to explore the state transition of neural activity when the animal starts planning a navigation route. Third, the behavioral test was conducted in darkness. Because visual identification of the spatial layout was not possible, the rats were required to rely on their internal map for navigation. These characteristics of the behavioral task helped us to investigate the neural mechanisms for navigational route planning in a rigorous manner.

A key finding in this dissertation is that RE inactivation resulted in impairment in navigation behavior as well as goal-directed trajectories represented by hippocampal CA1 neural ensemble activity. The correlation between the route planning impairment and the decrease in goal-directed trajectory events suggests that the RE projection is necessary for the role of hippocampal CA1 in route planning, which strengthens the previously proposed idea that trajectory sequences in the hippocampus support the planning of an upcoming journey. Together, my results suggest that the PFC-RE-CA1 circuitry plays a crucial role in the planning of navigational routes.

While I observed a navigation deficit following RE inactivation, RE neurons give rise to inputs in multiple brain regions. How can we say that this deficit is due to their projections to the hippocampus CA1? While a rigorous test would require a projection-specific manipulation, I found that the

bilateral hippocampal inactivation caused a similar route-planning deficit, as observed in the animals with RE inactivation, such as longer non-smooth navigational trajectories (*Chapter 4*). I further discovered that RE silencing impaired goal-directed trajectory sequences in the hippocampus. From these observations, the behavioral impairment in route planning is likely caused by abnormal hippocampal activity due to silenced RE inputs in hippocampal CA1.

How can hippocampal goal-directed trajectory events support obstacle avoidance route planning? One possibility is that these sequences may support a navigation strategy relying on subgoal identifications to reach a hidden final goal location in a complex environment (Redish, 1999; Trullier & Meyer, 2000; Spiers & Gilbert, 2015; Shamash et al., 2021). In the maze design in this project, the two edges of the inserted wall could be used as subgoals because rats always have to pass one of the wall edges to reach the goal location in the maze. The change in a behavioral trajectory following the first wall insertion in the maze may be associated with the animal's development of a strategy to target a subgoal. This subgoal strategy implies that hippocampal trajectory sequences may also represent a subgoal (wall edges) together with the final goal (a home well). Goal-directed trajectory sequences generated in the hippocampus may be essential for guiding the animal to create smooth obstacle-avoidance paths in the complex environment. This idea is consistent with my observation that goal-directed trajectory events can avoid the inserted wall (*Chapter 5*). These results are also in line with the previous work showing that trajectory sequences avoid a wall rather than penetrate through it (Widloski & Foster, 2022). A possible

reason why the trajectory events do not pass through a wall is the need for the brain to recognize wall edges as a plausible subgoal for navigation. However, such subgoal representation is not necessary for navigation in an open arena, which may be the reason why the navigation performance in the open maze was not affected by the absence of goal-directed trajectory events in the hippocampus.

However, while the dissertation addressed the behavioral and functional impact of the projections from the RE to the hippocampal CA1, it is still unclear how exactly the activity of RE neurons can influence the contents of trajectory sequences in the hippocampus. To address this question, I have been recording the activity of RE neurons using a Neuropixel probe while the animal performs the same task. Further analysis of the RE recording data could clarify how the activity of RE neurons can influence goal-directed trajectory sequences in the hippocampus.

The RE is located in the midline thalamus also in humans (Reeders et al., 2022), which exhibited pathological changes in patients with Alzheimer's disease (Braak & Braak, 1991) and major depressive disorder (Brown et al., 2017). Consistent with the role of the RE in navigation, patients with Alzheimer's disease showed difficulty in using allocentric cues for navigation (Parizkova et al., 2018). It is also reported that patients with major depression tend to take a longer path to reach a hidden goal destination (Cornwell et al., 2010). Because the brain’s abnormalities associated with Alzheimer's disease and depression disorder are not necessarily exclusive to the RE, but also other brain regions including the hippocampus, it is difficult to conclude a causal impact of the RE here. However, the result of this dissertation suggests that

RE could potentially be a therapeutic target to restore the navigation ability of these patients.

References

Adler, J. (1966). Chemotaxis in Bacteria. Science, 153, 708-716

Alyan, S., & McNaughton, B. L. (1999). Hippocampectomized rats are capable of homing by path integration. Behavioral Neuroscience, 113(1), 19–31.

Armbruster, B. N., Li, X., Pausch, M. H., Herlitze, S., Roth, B. L. (2007). Evolving the lock to fit the key to create a family of G protein-coupled receptors potently activated by an inert ligand. Proceedings of the National Academy of Sciences of the United States of America, 104(12), 5163 5168.

Avens, L., Lohmann, K. J. (2004). Navigation and seasonal migratory orientation in juvenile sea turtles. Journal of Experimental Biology, 207(11), 1771 1778.

Basu, R., Gebauer, R., Herfurth, T., Kolb, S., Golipour, Z., Tchumatchenko, T., Ito, H. T. (2021). The orbitofrontal cortex maps future navigational goals. Nature, 599(7885), 449 452.

Berndt, A., Lee, S. Y., Wietek, J., Ramakrishnan, C., Steinberg, E. E., Rashid, A. J., Kim, H., Park, S., Santoro, A., Frankland, P. W., Iyer, S. M., Pak, S., Delp, S. L., Malenka, R. C., Josselyn, S. A., Carlén, M., Hegemann, P., & Deisseroth, K. (2016). Structural foundations of optogenetics: Determinants of channelrhodopsin ion selectivity. Proceedings of the National Academy of Sciences, 113(4), 822-829.

Bokor, H., Csáki, Á., Kocsis, K., & Kiss, J. (2002). Cellular architecture of the nucleus reuniens thalami and its putative aspartatergic/glutamatergic projection to the

hippocampus and medial septum in the rat. European Journal of Neuroscience, 16(7), 1227-1239.

Braak, H., Braak, E. (1991). Alzheimer s disease affects limbic nuclei of the thalamus. Acta Neuropathologica, 81(3), 261 268.

Brown, E. C., Clark, D. L., Hassel, S., MacQueen, G., & Ramasubbu, R. (2017). Thalamocortical connectivity in major depressive disorder. Journal of Affective Disorders, 217, 125-131.

Cassel, J. C., Pereira de Vasconcelos, A., Loureiro, M., Cholvin, T., Dalrymple-Alford, J. C., Vertes, R. P. (2013). The reuniens and rhomboid nuclei: Neuroanatomy, electrophysiological characteristics and behavioral implications. Progress in Neurobiology, 111, 34 52.

Cholvin, T., Loureiro, M., Cassel, R., Cosquer, B., Geiger, K., De Sa Nogueira, D., Cassel, J.- C. (2013). The Ventral Midline Thalamus Contributes to Strategy Shifting in a Memory Task Requiring Both Prefrontal Cortical and Hippocampal Functions. Journal of Neuroscience, 33(20), 8772 8783.

Ciaramelli, E. (2008). The role of ventromedial prefrontal cortex in navigation: A case of impaired wayfinding and rehabilitation. Neuropsychologia, 46(7), 2099 2105. Collett, T. S., Collett, M., Wehner, R. (2001). The guidance of desert ants by extended landmarks. Journal of Experimental Biology, 204(9), 1635 1639.

Corkin, S. (1965). Tactually-guided maze learning in man: Effects of unilateral cortical excisions and bilateral hippocampal lesions. Neuropsychologia, 3(4), 339-351.

Corkin, S. (2002). What's new with the amnesic patient H.M.? Nature Reviews Neuroscience, 3(2), 153-160.

Cornwell, B. R., Salvadore, G., Colon-Rosario, V., Latov, D. R., Holroyd, T., Carver, F. W., Coppola, R., Manji, H. K., & Grillon, C. (2010). Abnormal hippocampal functioning and impaired spatial navigation in depressed individuals. The American Journal of Psychiatry, 167(7), 836.

Davoodi, F. G., Motamedi, F., Naghdi, N., Akbari, E. (2009). Effect of reversible inactivation of the reuniens nucleus on spatial learning and memory in rats using Morris water maze task. Behavioural Brain Research, 198(1), 130 135.

Diba, K., & Buzsáki, G. (2007). Forward and reverse hippocampal place-cell sequences during ripples. Nature Neuroscience, 10(10), 1241-1242.

Dolleman-van Der Weel, M.J. and Witter, M.P. (1996), Projections from the nucleus reuniens thalami to the entorhinal cortex, hippocampal field CA1, and the subiculum in the rat arise from different populations of neurons. J. Comp. Neurol., 364: 637-650.

Dolleman-Van Der Weel, M. J., Witter, M. P. (2000). Nucleus reuniens thalami innervates γ aminobutyric acid positive cells in hippocampal field CA1 of the rat. Neuroscience Letters, 278(3), 145 148.

Dolleman-Van Der Weel, M. J., Morris, R. G. M., Witter, M. P. (2009). Neurotoxic lesions of the thalamic reuniens or mediodorsal nucleus in rats affect non-mnemonic aspects of watermaze learning. Brain Structure and Function, 213(3), 329 342.

Foster, D. J., Wilson, M. A. (2006). Reverse replay of behavioural sequences in hippocampal place cells during the awake state. Nature, 440(7084), 680 683.

Hafting, T., Fyhn, M., Molden, S., Moser, M., Moser, E. I. (2005). Microstructure of a spatial map in the entorhinal cortex. Nature, 436(7052), 801 806.

Hardcastle, K., Ganguli, S., Giocomo, L. M. (2015). Environmental Boundaries as an Error Correction Mechanism for Grid Cells. Neuron, 86(3), 827 839.

Hartley, T., Maguire, E. A., Spiers, H. J., Burgess, N. (2003). The well-worn route and the path less traveled: Distinct neural bases of route following and wayfinding in humans. Neuron, 37(5), 877 888.

Herkenham, M. (1978). The connections of the nucleus reuniens thalami: Evidence for a direct thalamo-hippocampal pathway in the rat. Journal of Comparative Neurology, 177(4), 589-609.

Ito, H. T., Zhang, S., Witter, M. P., Moser, E. I., Moser, M. (2015). A prefrontal thalamo hippocampal circuit for goal-directed spatial navigation. Nature, 522(7554), 50 55.

Layfield, D. M., Patel, M., Hallock, H., Griffin, A. L. (2015). Inactivation of the nucleus reuniens/rhomboid causes a delay-dependent impairment of spatial working memory. Neurobiology of Learning and Memory, 125, 163 167.

Lee, A. K., & Wilson, M. A. (2002). Memory of Sequential Experience in the Hippocampus during Slow Wave Sleep. Neuron, 36(6), 1183-1194.

Lohmann, K. J., Lohmann, C. M. F., Ehrhart, L. M., Bagley, D. A., Swing, T. (2004). Geomagnetic map used in sea-turtle navigation. Nature, 428(6986), 909 910.

Loureiro, M., Cholvin, T., Lopez, J., Merienne, N., Latreche, A., Cosquer, B., Pereira de Vasconcelos, A. (2012). The ventral midline thalamus (reuniens and rhomboid nuclei) contributes to the persistence of spatial memory in rats. The Journal of Neuroscience: The Official Journal of the Society for Neuroscience, 32(29), 9947 9959.

Maguire, E. A., Gadian, D. G., Johnsrude, I. S., Good, C. D., Ashburner, J., Frackowiak, R. S., & Frith, C. D. (2000). Navigation-related structural change

in the hippocampi of taxi drivers. Proceedings of the National Academy of Sciences, 97(8), 4398-4403.

McKenna, J. T., Vertes, R. P. (2004). Afferent projections to nucleus reuniens of the thalamus. Journal of Comparative Neurology, 480(2), 115 142.

Milner, B. (1965). Visually-guided maze learning in man: Effects of bilateral hippocampal, bilateral frontal, and unilateral cerebral lesions. Neuropsychologia, 3(4), 317-338.

Mittelstaedt, M. L., Mittelstaedt, H. (1980). Homing by path integration in a mammal. Naturwissenschaften, 67(11), 566 567.

Muller, M., Wehner, R. (1988). Path integration in desert ants, Cataglyphis fortis. 85, 5287 5290.

Nagai, Y., Miyakawa, N., Takuwa, H., Hori, Y., Oyama, K., Ji, B., Minamimoto, T. (2020). Deschloroclozapine, a potent and selective chemogenetic actuator enables rapid neuronal and behavioral modulations in mice and monkeys. Nature Neuroscience, 23(9), 1157 1167.

O Keefe, J. (1976). Place units in the hippocampus of the freely moving rat. Experimental Neurology, 51(1), 78 109.

O Keefe, J., Dostrovsky, J. (1971). The hippocampus as a spatial map. Preliminary evidence from unit activity in the freely-moving rat. Brain Research, 34(1), 171 175.

Olsen, R. K., Palombo, D. J., Rabin, J. S., Levine, B., Ryan, J. D., Rosenbaum, R. S. (2013). Volumetric analysis of medial temporal lobe subregions in developmental amnesia using high-resolution magnetic resonance imaging. Hippocampus, 23(10), 855 860.

Pachitariu, M., Steinmetz, N., Kadir, S., Carandini, M., Harris, K. (2016). Fast and accurate spike sorting of high-channel count probes with KiloSort. Advances in Neural Information Processing Systems, (Nips), 4455 4463.

Parizkova, M., Lerch, O., Moffat, S. D., Andel, R., Mazancova, A. F., Nedelska, Z., Vyhnalek, M., Hort, J., & Laczó, J. (2018). The effect of Alzheimer's disease on spatial navigation strategies. Neurobiology of Aging, 64, 107-115.

Pfeiffer, B. E., Foster, D. J. (2013). Hippocampal place-cell sequences depict future paths to remembered goals. Nature, 497(7447), 74 79.

Redish, a D. (1999). Beyond the Cognitive Map: From Place Cells to Episodic Memory.

Reeders, P. C., Rivera Núñez, M. V., Vertes, R. P., Mattfeld, A. T., Allen, T. A. (2023). Identifying the midline thalamus in humans in vivo. Brain Structure and Function, 228(8), 1835-1847.

Rosenbaum, R. S., Winocur, G., Binns, M. A., & Moscovitch, M. (2012). Remote spatial memory in aging: All is not lost. Frontiers in Aging Neuroscience, 4.

Rosenbaum, R. S., Cassidy, B. N., Herdman, K. A. (2015). Patterns of preserved and impaired spatial memory in a case of developmental amnesia. Frontiers in Human Neuroscience, 9(MAY), 1 15.

Shamash, P., Olesen, S. F., Iordanidou, P., Campagner, D., Banerjee, N., Branco, T. (2021). Mice learn multi-step routes by memorizing subgoal locations. Nature Neuroscience, 24(9), 1270 1279.

Skaggs, W. E., McNaughton, B. L., Wilson, M. A., Barnes, C. A. (1996). Theta phase precession in hippocampal neuronal populations and the compression of temporal sequences. Hippocampus, 6(2), 149 172.

Spiers, H. J., Gilbert, S. J. (2015). Solving the detour problem in navigation: A model of prefrontal and hippocampal interactions. Frontiers in Human Neuroscience, Vol. 9.

Teng, E., & Squire, L. R. (1999). Memory for places learned long ago is intact after hippocampal damage. Nature, 400(6745), 675-677.

Tolman, E. C. (1948). THE PSYCHOLOGICAL REVIEW COGNITIVE MAPS IN RATS AND MEN (Vol. 55).

Trullier, O., Meyer, JA. (2000). Animat navigation using a cognitive graph. Biol Cybern. 83, 271–285

Vargha-Khadem, F., Gadian, D. G., Watkins, K. E., Connelly, A., Van Paesschen, W., Mishkin, M. (1997). Differential effects of early hippocampal pathology on episodic and semantic memory. Science, 277(5324), 376 380.

Vertes, R. (2002). Analysis of projections from the medial prefrontal cortex to the thalamus in the rat, with emphasis on nucleus reuniens. Journal of Comparative Neurology, 442(2), 163 187.

Vertes, R. P., Hoover, W. B., Szigeti-Buck, K., Leranth, C. (2007). Nucleus reuniens of the midline thalamus: Link between the medial prefrontal cortex and the hippocampus. Brain Research Bulletin, 71(6), 601 609.

Vertes, R. P., Linley, S. B., Rojas, A. K. P. (2022). Structural and functional organization of the midline and intralaminar nuclei of the thalamus. Frontiers in Behavioral Neuroscience, 16.

Viena, T. D., Linley, S. B., Vertes, R. P. (2018). Inactivation of nucleus reuniens impairs spatial working memory and behavioral flexibility in the rat. Hippocampus, 28(4), 297 311.

Widloski, J., Foster, D. J. (2022). Flexible rerouting of hippocampal replay sequences around changing barriers in the absence of global place field remapping. Neuron, 110(9), 1547-1558.e8.

Wood, E. R., Dudchenko, P. A., Robitsek, R. J., Eichenbaum, H. (2000). Hippocampal neurons encode information about different types of memory episodes occurring in the same location. Neuron, 27(3), 623 633.

Wouterlood, F. G., Saldana, E., Witter, M. P. (1990). Projection from the nucleus-reuniensthalami to the hippocampal region - light and electron-microscopic tracing study in the rat with the anterograde tracer phaseolus-vulgaris leukoagglutinin. Journal of Comparative Neurology, 296(2), 179 203

List of Abbreviations

AAV	Adeno-associated Virus
DCZ	Deschloroclozapine
DREADDs	Designer Receptors Exclusively Activated by Designer Drugs
E. coli	*Escherichia coli*
OFC	Orbitofrontal Cortex
PFC	Prefrontal Cortex
RE	Nucleus Reuniens of the thalamus
SEM	Standard Error of the Mean